

# RMP Colloquia

This section, offered as an experiment beginning in January 1992, contains short articles intended to describe recent research of interest to a broad audience of physicists. It will concentrate on research at the frontiers of physics, especially on concepts able to link many different subfields of physics. Responsibility for its contents and readability rests with the Advisory Committee on Colloquia, U. Fano, chair, Robert Cahn, S. Freedman, P. Parker, C. J. Pethick, and D. L. Stein. Prospective authors are encouraged to communicate with Professor Fano or one of the members of this committee.

## Quasicrystals and crystalline approximants

A. I. Goldman

*Ames Laboratory and Department of Physics and Astronomy, Iowa State University, Ames, Iowa 50011*

R. F. Kelton

*Department of Physics, Washington University, St. Louis, Missouri 63130*

Over the past seven years, many examples of periodic crystals closely related to quasicrystalline alloys have been discovered. These crystals have been termed *approximants*, since the arrangements of atoms within their unit cells closely approximate the local atomic structures in quasicrystals. This colloquium focuses on these approximant structures, their description, and their relationship to quasicrystals.

### CONTENTS

I. Introduction	213
II. Quasicrystals and Approximants	214
A. Quasicrystals	214
B. Prototypical crystalline approximants	216
C. Structural similarities between the icosahedral phase and cubic approximants	216
III. Describing the Structure of Quasicrystals and their Crystalline Approximants	219
A. Aperiodic structures and periodic approximants in one dimension	219
B. Quasicrystals and approximants in two and three dimensions	222
C. Observed rational approximants	225
IV. Using Crystalline Approximants to Model the Structure of Quasicrystals	226
V. Phase Transitions Between Approximants and Quasicrystals	227
VI. Electronic and Electron-Transport Properties of Quasicrystals and Approximants	228
VII. Concluding Remarks	228
Acknowledgments	229
References	229

### I. INTRODUCTION

The discovery of the icosahedral alloys (Shechtman *et al.*, 1984; Shechtman and Blech, 1985) has generated a great deal of excitement, as well as confusion, in many scientific circles. These intermetallic alloys belong to a growing class of materials known as “quasicrystals,” which may be defined as structures with long-range aperiodic order and crystallographically forbidden rotational symmetries (e.g., fivefold, eightfold, tenfold, and

12-fold rotation axes). The observation that certain intermetallic compounds produced sharp diffraction peaks displaying the “noncrystallographic” icosahedral rotational point group at first appeared to challenge the basic tenets of crystallography. This is, in fact, not true, since the traditional crystallographic classification schemes deal only with the periodic arrangements of atoms and the consequent allowed space groups. Quasicrystalline structures simply fall outside these boundaries. In a recent series of interesting reviews, however, crystallographic classifications have been recast into a broader, less restrictive framework that treats periodic and aperiodic crystals on an equal footing (Rabson *et al.*, 1991; Mermin, 1992).

Early debates over the interpretation of diffraction data from quasicrystals, led by Linus Pauling (1985),<sup>1</sup> raised several interesting issues that have become active areas of quasicrystal-related research. Perhaps the most fundamental of these relates to the limits of our ability to distinguish between a true quasicrystal and periodic crystals (possibly twinned) with complex large unit cells. Over the past seven years, structural similarities between known crystalline phases, such as  $\alpha(\text{AlMnSi})$ ,<sup>2</sup> and related quasicrystalline phases, [e.g., icosahedral  $i(\text{AlMnSi})$ ] have been explored in detail. Furthermore, many new examples of periodic crystals closely related to quasicrys-

<sup>1</sup>See the several responses to Pauling’s arguments in *Nature* **319**, 102 (1986).

<sup>2</sup>The designation  $\alpha(\text{AlMnSi})$  refers to one of several phases of the Al-Mn-Si ternary alloy.

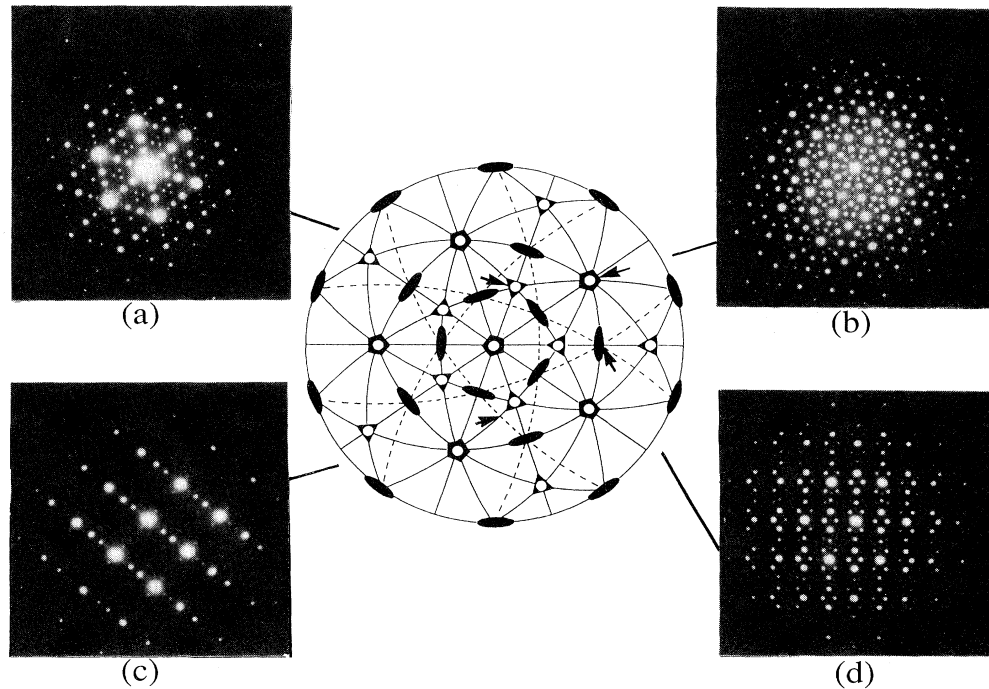


FIG. 1. Stereographic projection of the  $m\bar{3}5$  point group and accompanying TEM diffraction patterns from rapidly quenched Al-Mn taken perpendicular to a (a) a threefold axis, (b) a fivefold axis, (c) a pseudo-twofold axis, and (d) a twofold axis.

talline phases have been discovered. Termed “approximants,” because the arrangements of atoms within their unit cells closely approximate the local atomic structures in quasicrystals, these alloys have played an important role in efforts to describe the atomic scale structure of quasicrystals, their formation, stability, and physical properties.

While icosahedral quasicrystals have received the most attention, other classes of quasicrystals also exist. Axial quasicrystalline structures are aperiodic in a plane perpendicular to an axis along which there is translational periodicity. The decagonal phase of Al-Mn was announced within a few months of the discovery of icosahedral Al-Mn (Bendersky, 1985; Chattopadhyay *et al.*, 1985). Octagonal and dodecagonal quasicrystalline phases in transition-metal Si alloys have also been reported (Ishimasa *et al.*, 1985; Wang *et al.*, 1987; Chen *et al.*, 1988). All of these quasicrystals have crystalline counterparts that are closely related in composition and local atomic structure. While some references will be made to these other quasicrystals in this review, much of our discussion will be limited to the icosahedral alloys and their approximants.

There is now a vast literature on quasicrystals, and several recent review articles and reprint collections have summarized developments and issues in the field (DiVincenzo and Steinhardt, 1991; Goldman and Widom, 1991; Guyot *et al.*, 1991; Kelton, 1992). With some discussion of the key features of quasicrystal structure, this colloquium focuses on the related approximant structures, their description, and their relationship to quasicrystals.

## II. QUASICRYSTALS AND APPROXIMANTS

### A. Quasicrystals

It is well known that periodic arrangements of objects, such as atoms, admit only certain rotational operations about an axis which bring the arrangement back into registry with the unrotated assembly. For three-dimensional periodic crystals the allowed operations include twofold, threefold, fourfold, and sixfold rotations about appropriately chosen axes. Taken together with other operations such as translations, reflections, and inversions, these point-group operations define all of the 230 space groups.<sup>3</sup> Space groups that include fivefold, sevenfold, and higher-order rotational operations are explicitly excluded.

If we insist that only periodic arrangements of atoms can produce Bragg diffraction peaks, the patterns obtained from a rapidly quenched alloy of Al-Mn, shown in Fig. 1, cause a dilemma. The sharp diffraction spots in Fig. 1(b) clearly lie in a reciprocal space plane perpendicular to a fivefold axis. The set of angular displacements between twofold, threefold, and fivefold axes in Fig. 1 demonstrates that the alloy has the forbidden icosahedral point-group symmetry.

<sup>3</sup>Under the heading of translations, we include translations that are not in the Bravais lattice in order to account for non-symmorphic space groups which include operations involving screw axes and glide planes, for example.

The resolution of this dilemma begins with the realization that Bragg diffraction does not require long-range periodic translational order, but rather *long-range positional order*,<sup>4</sup> which may or may not be specified by a periodic function in three dimensions. In this sense, quasicrystals may be viewed as incommensurate<sup>5</sup> structures. Quasicrystals, however, differ from traditional incommensurate structures because they have noncrystallographic rotational symmetries. A careful inspection of the sequence of diffraction spots along any axis of the patterns in Fig. 1 shows that the ratio of distances from the origin to any two bright spots is an irrational number within reasonable experimental error. For icosahedral quasicrystals, this irrational number is some power of the golden mean  $\tau$  [ $\tau = 2 \cos(\pi/10) = (1 + \sqrt{5})/2$ ], which arises from the geometries of icosahedra, pentagons, and decagons. A related interesting property of the diffraction patterns in Fig. 1 is that while they do not have translational symmetry, they do have inflation symmetry. That is, the diffraction patterns in Fig. 1, for example, can be expanded or contracted by a factor of  $\tau^3$  to yield patterns indistinguishable from the originals. The fact that Bragg diffraction is possible from aperiodic structures is no longer the subject of greatest interest. The key issue is what do these diffraction patterns imply about the underlying structure of a quasicrystal?

The absence of periodicity confounds many of the important ideas and methods that are used to describe the structure and properties of ordered solids. While, as we shall discuss later, atomic motifs or clusters that are found frequently in quasiperiodic structures exist, the concept of a fundamental "unit cell"<sup>6</sup> is lost. In the same vein, calculations of electronic and vibrational properties of periodic crystals are vastly simplified by the concept of a Brillouin zone, which, again, is inappropriate for quasicrystals. It is worth emphasizing here, however, that quasicrystalline alloys should not be viewed as disordered or glassy materials. Indeed, if the peak widths measured in x-ray-diffraction experiments are taken as a measure of the range of positional coherence, there are several examples of quasicrystals that are as well ordered as typical crystalline intermetallic alloys (Bancel, 1989; Guryan *et al.*, 1989).

The intrinsic incommensurability of the icosahedral phase complicates the description of both its structure in physical space and the reciprocal space distribution of in-

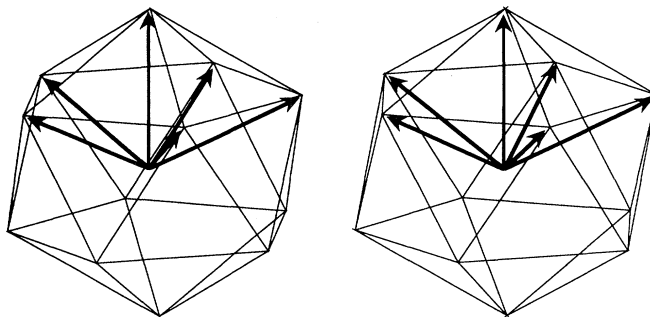


FIG. 2. Stereogram of an icosahedron and a set of possible basis vectors for indexing icosahedral quasicrystals. A 3D image can be viewed by staring at a point between the two icosahedra and slowly crossing your eyes.

tensity in scattering measurements. For example, an attempt at indexing the diffraction patterns in Fig. 1 in terms of the three Miller indices ( $hkl$ ) used for conventional crystalline structures leads to irrational indices rather than integer values. As implied by the icosahedral symmetry of the diffraction patterns, the appropriate basis set for indexing icosahedral quasicrystal diffraction patterns is defined by the six unique vectors that point from the center to the vertices of an icosahedron, as shown in Fig. 2. This means that each reciprocal-lattice vector (diffraction peak) requires six indices for integer indexing (Bancel *et al.*, 1985; Elser, 1985a).<sup>7</sup> The fact that six indices are required for indexing the diffraction patterns of icosahedral alloys is also intimately related to the proper approach for obtaining a description of the real-space structure using conventional crystallographic techniques. For icosahedral quasicrystals, one definition of the reciprocal-lattice vectors is given by

$$\mathbf{G}_i^{\parallel} = g_0 \sum_{i=1}^6 n_i \hat{\mathbf{e}}_i^{\parallel}, \quad (1)$$

$$\hat{\mathbf{e}}_i^{\parallel} = \frac{1}{(1 + \tau^2)^{1/2}} \begin{pmatrix} 1 & \tau & 0 \\ -1 & \tau & 0 \\ 0 & 1 & \tau \\ \tau & 0 & 1 \\ \tau & 0 & -1 \\ 0 & 1 & -\tau \end{pmatrix} \begin{pmatrix} \hat{\mathbf{i}} \\ \hat{\mathbf{j}} \\ \hat{\mathbf{k}} \end{pmatrix},$$

where the  $\hat{\mathbf{e}}_i^{\parallel}$  are the basis vectors mentioned above, the  $n_i$  are integers, and  $g_0$  is a constant that sets the scale of the diffraction pattern. Because of the inflation symmetry, no single fundamental length ( $g_0$ ) can be chosen *ab initio*. For periodic crystals, a fundamental length scale is dictated by the unit-cell edge lengths [e.g., for cubic crystals, the (100) reflection is found at wave vector  $2\pi/a$  along the  $h00$  axis, where  $a$  is the lattice constant]. For quasicrystals, the concept of a *quasilattice constant* is not as clearly defined by the diffraction pattern.

<sup>4</sup>Well-ordered structures can arise from the application of rules governing the sequence of operations used to build the structure. An example of this in one dimension, the Fibonacci sequence, is described in Sec. III.

<sup>5</sup>Incommensurate structures lack periodic translational order because two or more elements of translational symmetry that are mutually incompatible are present.

<sup>6</sup>A unit cell is the smallest structural element of a periodic crystal that, when translated through the vectors of the Bravais lattice, reproduces the crystal structure.

<sup>7</sup>An alternative indexing scheme has been presented by Cahn, Shechtman, and Gratias (1986).

Two types of icosahedral quasilattices have been observed. For simple icosahedral (SI) structures, such as those found in Al-Mn, Al-Li-Cu (Ball and Lloyd, 1985; Sainfort *et al.*, 1985), Ga-Mg-Zn (Chen and Inoue, 1987), and Ti-Mn-Si (Kelton *et al.*, 1988), the indices are unrestricted (each  $n_i$  may take on any integer value), in analogy with simple cubic crystals. For face-centered icosahedral (FCI) structures, such as Al-Cu-Fe, Al-Cu-Ru (Tsai *et al.*, 1988), and Al-Pd-Mn (Tsai *et al.*, 1990), the indices must have the same parity ( $n_i$  all even or all odd), in analogy with face-centered-cubic crystals. Interestingly, there are striking differences in the stability and degree of disorder between these two classes of alloys that appear to be related to an enhanced degree of chemical order in the FCI alloys. Structural differences between FCI and SI alloys have been the subject of intense scrutiny over the past three years.

### B. Prototypical crystalline approximants

If the goal is to understand the structure of quasicrystals (in particular the icosahedral phase), why study crystalline approximants? The many reasons include the facts that (1) quasicrystals typically form at compositions near those of crystalline approximant phases; (2) the approximants provide a well-defined starting point for models of the local atomic structure of quasicrystals; and (3) both quasicrystalline and approximant phases have similar physical properties. Those of the approximants may be easier to understand theoretically, since all of the calculational mechanisms established for periodic crystals may be applied more readily to them. All of these points are, of course related. The compositional similarities between quasicrystals and their respective approximants, for example, suggest a similarity in their local atomic structures substantiated by similarities in physical properties. Approximants are important for studies of formation and stability, since they are more amenable to established theoretical tools, such as band-structural calculational techniques. Reversible transformations between quasicrystals and related crystalline approximant structures have been observed and studied in some detail over the past two years. Furthermore, in some samples, the quasicrystalline and approximant phases often coexist in orientational epitaxy. In a real sense, then, crystalline approximants are the missing link between quasicrystals and periodic crystals. In this section we describe the structure of two prototypical crystalline approximants to the icosahedral phase alloys.

Many complex crystalline structures contain large clusters of atoms that are arranged in a near-perfect tetrahedral coordination. These clusters are frequently connected by other polyhedral atomic clusters. Perhaps the simplest example of this is the body-centered-cubic (bcc) structure of  $\text{MoAl}_{12}$  (see Pearson, 1972) containing identical icosahedral clusters centered at the origin and body center of the unit cell, linked by an octahedron that shares opposite faces with both. In  $\text{MoAl}_{12}$ , these

icosahedra contain 12 Al atoms on the vertices and one Mo atom at the cluster center. A nearly identical construction is found in  $\alpha(\text{AlMnSi})$  (Cooper and Robinson, 1966), a simple cubic phase that is closely related to the icosahedral phase (*i*-phase) in Al-Mn-Si alloys. Here, however, the basic structural unit is the 54-atom Mackay icosahedron (Mackay, 1962), shown in Fig. 3. It consists of an empty core surrounded by 12 Al atoms at the vertices of an icosahedron, 12 Mn atoms beyond the original 12 Al atoms, and 30 Al atoms sitting on the twofold positions (icosahedron edge centers) defined by the Mn sites. As in  $\text{MoAl}_{12}$ , the Mackay icosahedra at the corners of the cube are connected to those at the body center along the threefold axes of the icosahedra by octohedra of Al atoms from the edges of two opposing triangular faces (Fig. 3). In reality, the icosahedral clusters in  $\alpha(\text{AlMnSi})$  are distorted by the cubic environment, clusters at the corners and body center being slightly different, and additional Al atoms being found between second-nearest-neighbor clusters along the  $\langle 100 \rangle$  directions. A bcc version of this phase,  $\alpha(\text{TiCrSi})$  (Libbert *et al.*, 1992), is related to the *i*-phase in Ti-TM-Si alloys, where TM = V, Cr, Mn, or Fe.

The Frank-Kasper phases (Frank and Kasper, 1958, 1959) are a particularly interesting class of structure, since they are tetrahedrally close packed containing only tetrahedral interstitial sites. Their structures are layered, with four layers per lattice repeat distance along one direction—two main layers and two subsidiary layers of lower atomic density. The main layers consist of pentagons and/or hexagons and triangles; the subsidiary layers consist of squares or rectangles and triangles. These phases are typically found in transition-metal alloys. Generally, the smaller atoms occupy the icosahedral sites and the larger atoms sit in sites of nonicosahedral coordination, accommodating the frustration that arises from packing icosahedra. The Bergman phase,  $\text{Mg}_{32}(\text{Al}, \text{Zn})_{49}$  (Bergman *et al.*, 1957), and the isomorphous  $\text{Al}_5\text{CuLi}_3$  (Cherkashin *et al.*, 1963; Guryan *et al.*, 1988) structures (bcc, space group  $\text{Im}\bar{3}$ ) are Frank-Kasper phases that are closely related to the icosahedral phases that form in those two alloys. Both of these structures are characterized by bcc packings of Pauling triacontahedral clusters of atoms, as shown in Fig. 3. In contrast to the distribution of atomic sites in  $\alpha(\text{AlMnSi})$ , virtually all of the atoms in the cubic unit cell are found in these clusters.

### C. Structural similarities between the icosahedral phase and cubic approximants

A preponderance of evidence suggests strong structural similarities between these crystalline phases and their respective quasicrystals. The most intense peaks in the crystalline approximant diffraction patterns, for example, correspond to the locations of prominent peaks of the related quasicrystal. Furthermore, quasicrystals frequently form with compositions near those of approximants. For

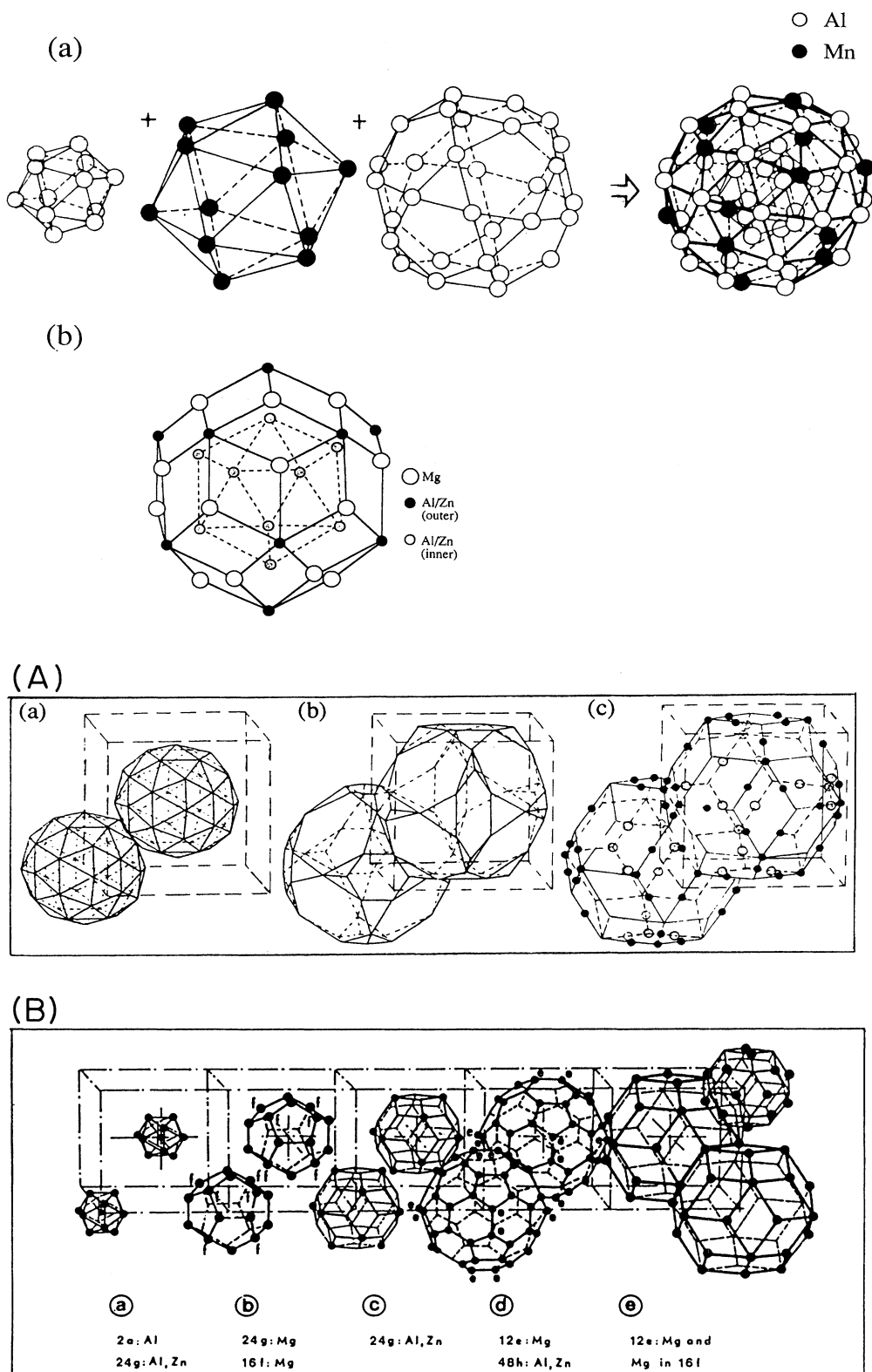


FIG. 3. Cubic crystalline approximants to the icosahedral alloys. Top: (a) construction of the 54-atom Mackay icosahedron of Al (white) and Mn (black) atoms (from Audier and Guyot, 1989); (b) the Pauling triacontahedral cluster (from Mukhopadhyay *et al.*, 1989). Bottom: (A) near-bcc packing of Mackay icosahedra in  $\alpha(\text{AlMnSi})$ ; (B) bcc packing of Pauling triacontahedra in the Bergman phase (from Audier and Guyot, 1989).

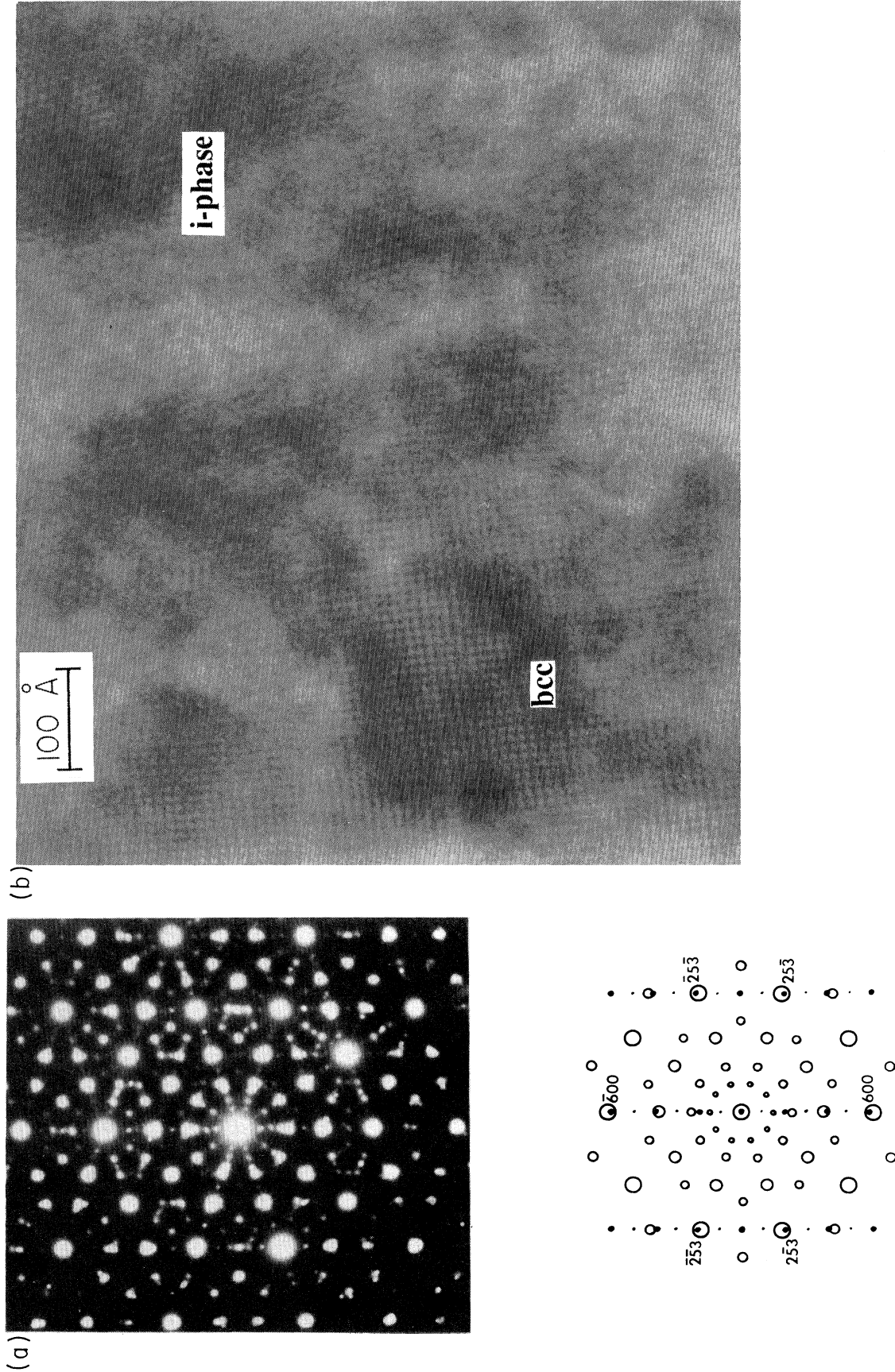


FIG. 4. Coherent orientational relationships between icosahedral phases and crystalline approximants. (a) Top: overlapping diffraction patterns of the fivefold zone of  $i(\text{AlMnSi})$  and the (530) zone of  $\alpha(\text{AlMnSi})$  (courtesy of H. S. Chen, taken from Koskenmaki *et al.*, 1986); bottom: schematic view of the top panel labeled with indices for the  $\alpha(\text{AlMnSi})$  diffraction spots. (b) High-resolution electron micrograph of coherent phase growth of the icosahedral and bcc phase of Ti-V-Si (from Zhang and Kelton, 1992).

example, the “best”  $i(\text{AlMnSi})$  composition is  $\text{Al}_{74}\text{Mn}_{20}\text{Si}_6$ , yielding sharp diffraction peaks, more uniform contrast in transmission electron microscope (TEM) images, and a crystallization temperature almost  $200^\circ\text{C}$  higher than at other compositions (Chen and Chen, 1986). This composition is very near to that of  $\alpha(\text{AlMnSi})$ ,  $\text{Al}_{72.5}\text{Mn}_{17.4}\text{Si}_{10.3}$ . One of the most successful approaches to finding new quasicrystals, in fact, is to search for crystalline approximants. The first quasicrystal discovered in an alloy with no transition metals,  $i(\text{AlMgZn})$ , was found by quenching an alloy at the composition of the Bergman phase. (Ramachandrarao and Sastry, 1985; Mukhopadhyay *et al.*, 1985).

One of the most convincing pieces of evidence for structural similarity is the frequent occurrence of the  $i$ -phase and the crystal approximant growing coherently together in the same sample. Figure 4(a), for example, displays a diffraction pattern taken from an  $i(\text{AlMnSi})$  alloy that also contains cubic  $\alpha(\text{AlMnSi})$  (Koskenmaki *et al.*, 1986). The planes perpendicular to a fivefold axis of  $i(\text{AlMnSi})$  and the (350) zone axis of the cubic  $\alpha(\text{AlMnSi})$  approximately overlap. Diffraction patterns taken along other zone axes demonstrate the alignment of prominent crystallographic directions:  $\langle 100 \rangle_{\text{bcc}}$ /twofold  $i$ -phase, and  $\langle 111 \rangle_{\text{bcc}}$ /threefold  $i$ -phase. Coherent phase boundaries can be found frequently in TEM images of the phase mixture, as demonstrated in Fig. 4(b) for  $i(\text{TiVSi})$  (Zhang and Kelton, 1991). Similar orientational relations have also been reported for  $i(\text{TeFeSi})$  and a bcc phase now known to be nearly isostructural with  $\alpha(\text{AlMnSi})$  (Dong *et al.*, 1987), and between the  $i$ -phase and the Bergman phase in Al-Mg-Zn alloys (Audier *et al.*, 1986).

### III. DESCRIBING THE STRUCTURE OF QUASICRYSTALS AND THEIR CRYSTALLINE APPROXIMANTS

As is true for any solid, the structures of quasicrystals can be described by an atomic density  $\rho(\mathbf{r})$ , which can be expanded as a Fourier series:

$$\rho(\mathbf{r}) = \sum_{\mathbf{Q}} \rho_{\mathbf{Q}} \exp(i\mathbf{Q} \cdot \mathbf{r}). \quad (2)$$

For periodic three-dimensional crystals, the wave vectors ( $\mathbf{Q}$ ) in the expansion can be taken as the lattice vectors of the reciprocal lattice, resulting in an atomic density periodic in three dimensions. For an icosahedral quasicrystal, the set of basis vectors pointing from the center to the vertices of an icosahedron are chosen, resulting in a density function periodic in six, rather than three, dimensions. This description is not a truly novel innovation, since such higher-dimensional treatments of incommensurate structures have been used for many years (see, for example, de Wolff, 1974 and Janner and Janssen, 1977). One of the most active areas in quasicrystal research over the past five years has been crystallography in six dimensions, using standard crystallographic tech-

niques to describe the atomic basis in higher dimensions.

The problem remains that quasicrystals and their crystalline approximants are inherently three-dimensional structures. Indeed, much can be learned about the local atomic configurations in quasicrystals by studying the occurrence of various local environments in the related approximant phases. To illustrate their close relationship on a more global scale, however, we shall use a technique termed *cut and projection*, which makes use of the higher-dimensional description of quasicrystalline structure (de Bruijn, 1981; Kramer and Neri, 1984; Bak, 1985a, 1985b; Duneau and Katz, 1985; Kalugin *et al.*, 1985; Elser, 1986).

#### A. Aperiodic structures and periodic approximants in one dimension

The 2D to 1D projection, described below, provides a useful illustration of the cut and projection formalism, as well as a means for describing the structure of experimentally observed 1D incommensurate structures that are closely related to quasicrystal approximants. One-dimensional “quasicrystals” have been reported in Al-Cu-Co, Al-Ni-Si, and Al-Cu-Mn (He *et al.*, 1988). The in-plane structure of these layered materials is *periodic*, while the planes themselves are stacked aperiodically in a Fibonacci sequence, which is a series that can be generated by the simple inflation rule illustrated in Fig. 5. Each successive generation of the sequence is constructed from the concatenation of the previous two generations or, equivalently, long segments ( $l$ ) and short segments ( $s$ ) in each generation become ( $ls$ ) and ( $l$ ) segments, respectively, in the next.

The closely related crystalline  $\tau$  phases are a series of vacancy-ordered CsCl structures with repeat distances along the  $\langle 111 \rangle$  directions that approximate a Fibonacci sequence (Chattopadhyay *et al.*, 1987). In Al-Ni-Cu, for example,  $\tau_2$ ,  $\tau_3$ ,  $\tau_5$ ,  $\tau_8$ ,  $\tau_{13}$ ,  $\tau_{21}$ , and  $\tau_{34}$  variants have been identified (Amelinckx *et al.*, 1990), where the subscript denotes the number of layers in the repeat unit. These numbers are members of the Fibonacci sequence defined by the recursion relation  $F_{n+1} = F_n + F_{n-1}$ . The one-dimensional Fibonacci structure may be denoted by  $\tau_n$  in the limit  $n \rightarrow \infty$ .

Figure 6(a) details the prescription for obtaining an

S	1
L	1
LS	2
LSL	3
LSLLS	5
LSLLSLSL	8
LSLLSLSLLS	13
LSLLSLSLLSLSLLS	21

FIG. 5. Generation of a Fibonacci sequence by the rule ( $l \rightarrow ls$ ;  $s \rightarrow l$ ). The Fibonacci numbers on the right-hand side count the number of members in a particular generation.

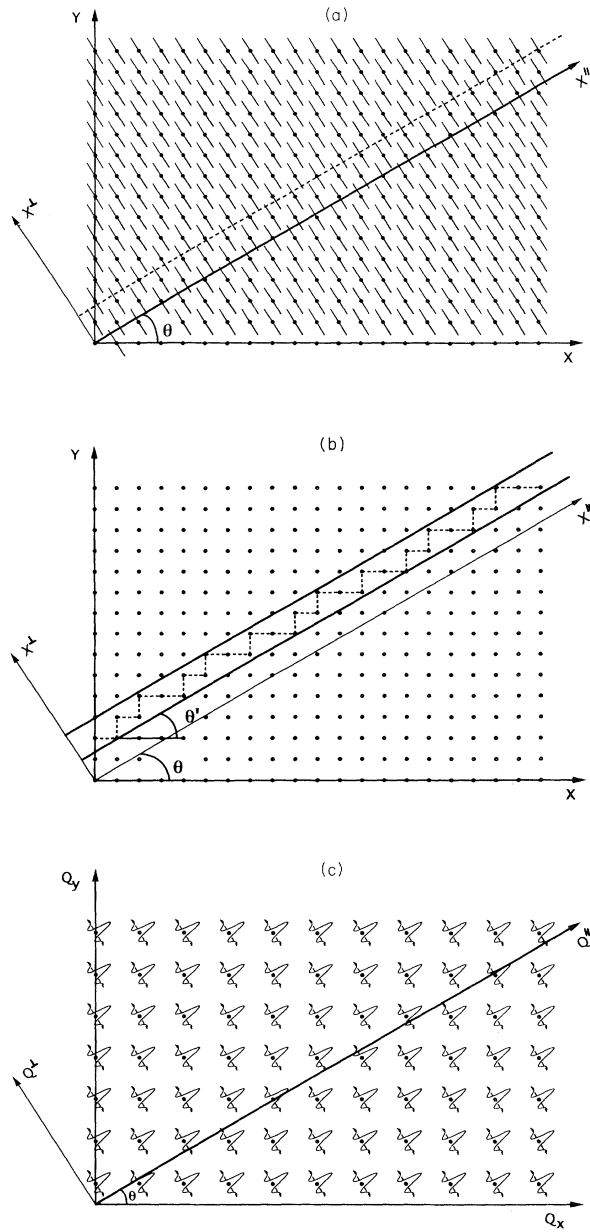


FIG. 6. Constructing a Fibonacci sequence by cut and projection. (a) The line segments represent atomic surfaces at sites of a two-dimensional square lattice. The intersections of the atomic surfaces with the one-dimensional physical space  $X^{\parallel}$  place atoms in a Fibonacci sequence. The dashed line represents a rigid shift of the  $X^{\parallel}$  axis along the  $X^{\perp}$  direction. (b) An alternative scheme constructs a Fibonacci sequence of atoms in one dimension. The heavy lines represent the boundaries of an acceptance domain. All sites in the 2D lattice within the boundaries are projected onto  $X^{\parallel}$ . The horizontal and vertical dashed lines project onto  $l$  and  $s$  segments along the  $X^{\parallel}$  axis. (c) An expanded view of the Fourier transform of the Fibonacci sequence is obtained by placing the Fourier transform of the surfaces in (a), or the acceptance domain in (b), at the sites of a two-dimensional lattice reciprocal to those of (a) and (b). The intensity of a diffraction peak is proportional to the square of the amplitude of the transforms where it intersects the  $Q^{\parallel}$  axis.

aperiodic array of atoms in one dimension from a periodic square lattice in two dimensions. We introduce a second set of axes rotated by some angle  $\theta$  with respect to the axes of the square lattice. The axis of most immediate interest, the physical space where our one-dimensional atomic array appears, is labeled as  $X^{\parallel}$ , while its orthogonal partner is denoted by  $X^{\perp}$ . In order to produce pointlike atoms in the physical space, the atomic basis in two dimensions can be represented by extended objects, such as the heavy line segments of length  $L$  perpendicular to  $X^{\parallel}$  shown in Fig. 6(a). The intersection of the basis with the  $X^{\parallel}$  axis locates the position of atoms in the physical space. The physical space, then, represents a one-dimensional *cut* through the two-dimensional periodic lattice.

An alternate, but less general, construction that is useful in many cases ignores the details of the atomic basis, choosing instead an *acceptance domain* such that all of the lattice points inside the acceptance domain are *projected* onto the physical space  $X^{\parallel}$ . This is illustrated by the heavy lines in Fig. 6(b), which define an acceptance domain of width  $L$  with the same orientation ( $\theta' = \theta$ ) as the  $X^{\parallel}$  axis. Incommensurate structures in one dimension result if  $\cot(\theta')$  is an irrational number. For instance, if  $\cot(\theta') = \tau$ , as shown for Fig. 6(b), the atomic density along  $X^{\parallel}$  is described by a Fibonacci sequence of long ( $l$ ) and short ( $s$ ) interatomic spacings that result from the projection of the horizontal and vertical dashed lines in the acceptance domain.

The diffraction pattern [Fig. 6(c)] resulting from this sequence can be computed through the Fourier transform of the atomic basis in Fig. 6(a), or the acceptance domain in Fig. 6(b), locating the points of intersection between the two-dimensional structure factor and the physical reciprocal space axis  $Q^{\parallel}$ . These points of intersection are the reciprocal-lattice vectors  $G^{\parallel}$ . Each diffraction peak has associated with it a value of  $G^{\parallel}$  and  $G^{\perp}$  (the component of the 2D reciprocal-lattice vector orthogonal to the physical space). In this simple example, the Fourier transform of the basis, or acceptance domain, results in a set of  $\delta$  functions along the  $Q^{\parallel}$  axis (at specific values of  $G^{\parallel}$ ) with an intensity given by  $[\sin(G^{\perp}L)/G^{\perp}L]^2$ .

Although the Fibonacci lattice constructed here is more properly classified as incommensurate rather than quasicrystalline (since the signature of a quasicrystal is the occurrence of noncrystallographic rotational symmetries), the cut and projection scheme illustrates the essential relationship between quasicrystals and crystalline approximants. Consider the situation depicted in Fig. 7. Here, the angle  $\theta = \cot^{-1}(\tau)$  between the  $X$  axis of the two-dimensional lattice and the rotated  $X^{\parallel}$  axis differs from the angle  $\theta' = \cot^{-1}(\frac{3}{2})$  that describes the orientation of the acceptance domain. By defining  $\cot(\theta) = \tau$ , the lengths of the  $l$  and  $s$  segments are constrained to be the same as those found for the aperiodic sequence constructed before. Projecting the points within the new acceptance domain onto the  $X^{\parallel}$  axis, we find that the result-

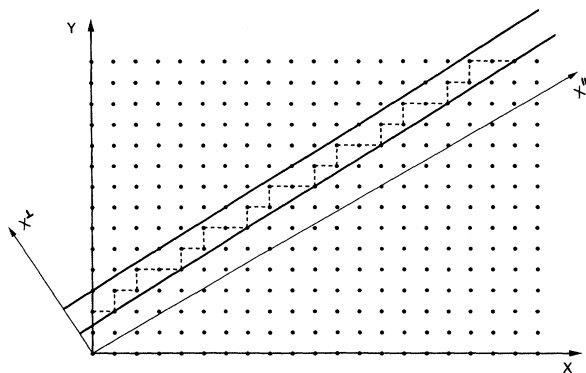


FIG. 7. A  $3/2$  rational approximant to the Fibonacci sequence, obtained by defining the angle of inclination of the acceptance domain so that  $\cot(\theta')=3/2$ . The periodic unit cell is composed of the sequence  $(lslls)$  projected from the sequence of horizontal ( $h$ ) and vertical ( $v$ ) dashed lines in the acceptance volume  $(hvhv)$ .

ing structure is a periodic sequence of the same segments found in the Fibonacci sequence with a repeat distance of  $(lslls)$ . This structure is the  $\frac{3}{2}$  rational approximant of the aperiodic Fibonacci sequence. We need not stop here. Periodic approximants to the Fibonacci sequence of larger and larger unit-cell dimensions may be produced with  $\cot(\theta')$  equal to any rational approximation of  $\tau$ ,  $F_{n+1}/F_n$ , where the  $F_n$  are the Fibonacci numbers. The diffraction patterns from these approximants will be similar to those of the Fibonacci sequence. The higher the order of the approximant, the larger the unit cell, and the more difficult it becomes to distinguish it from an aperiodic structure.

So far we have concentrated mainly on the physical-space axes of the rotated coordinate systems  $X^{\parallel}$  and  $Q^{\parallel}$ . Displacements of the structure along the  $X^{\parallel}$  direction correspond to displacements or translations in physical space. The hydrodynamic modes associated with these displacements are simply phonon modes. Distortions in the unit-cell dimension (physical strain) result in diffraction peak broadening that increases with  $G^{\parallel}$ .

What about displacements of the structure, or acceptance domain, along the orthogonal  $X^{\perp}$  direction in Figs. 6(a) and 6(b). A rigid translation of the  $X^{\parallel}$  axis in Fig. 6(a), or of the acceptance domain in Fig. 6(b), along the  $X^{\perp}$  direction will still result in a one-dimensional Fibonacci sequence along  $X^{\parallel}$ . As the dashed line in Fig. 6(a) shows, however, the arrangement of the  $l$  and  $s$  segments has changed. The diffraction pattern from this new structure is identical to the original one. The rigid shift along  $X^{\perp}$  has simply shifted our view of the structure by some distance along the  $X^{\parallel}$  axis. It is well known that incommensurate structures have additional degrees of freedom associated with the relative phases of the density waves (in a Landau description) that are not found in periodic crystals. These modes, associated with the displacements along the  $X^{\perp}$  axis, are termed *phason modes* (Bak, 1985a, 1985b; see also Lubensky, 1988).

Many of the models for quasicrystalline structures are differentiated by the description of the acceptance volume in higher dimensions. For example, two- and three-dimensional Penrose tilings result from projections of perfectly smooth, properly oriented acceptance domains [analogous to that of Fig. 6(b)] embedded in 5D and 6D hypercubic lattices, respectively. Penrose tilings were the first class of models employed to describe the structure of icosahedral alloys (Levine and Steinhardt, 1984, 1986).

The relative phase (phason) degrees of freedom for incommensurate structures are intimately connected to the relationship between quasicrystals and their crystalline approximants. We have already seen that rational approximants to the Fibonacci sequence may be generated by “locking in” the slope of the acceptance domain to a rational approximation of  $\tau$ . Other possibilities exist if the acceptance domain is allowed to meander through the higher-dimensional periodic lattice, as shown in Fig. 8.

In Fig. 8(a), the slope of the acceptance domain fluctuates about an average value equal to  $\tau^{-1}$ . The fluctuations are bounded and result in a structure that is a Fibonacci sequence, on average, with some local defects. The diffraction pattern from such a structure consists of Bragg peaks at the same positions as those of the Fibonacci structure along with some diffuse scattering from the defects. This description forms the basis of “random-tiling” models for quasicrystals (Elser, 1985b; Henley, 1988; Strandburg *et al.*, 1989; Widom *et al.*, 1989).

The disorder produced by the meandering acceptance domain in Fig. 8(b) is much more severe. These fluctuations are unbounded (i.e., grow as  $X^{\parallel}$  increases) and can produce randomized sequences of  $l$  and  $s$  segments. Disordered structural models for the icosahedral alloys, such as the “icosahedral-glass” model (Shechtman and Blech, 1985; Stephens and Goldman, 1986; Elser, 1987; Robertson and Moss, 1991), may be described in this manner. More generally, the disorder generated in this manner has been termed *phason strain* (Socolar and Wright, 1987; Lubensky, 1988). The diffraction patterns from such structures will consist of relatively sharp peaks with line shapes, widths, and positions depending upon the details of the fluctuations. The signature of phason strain in a quasicrystal is the observation of shifts in the position and/or broadening of diffraction peaks which are independent of  $G^{\parallel}$ , but increasing with  $G^{\perp}$ . Almost all of the quasicrystals studied before 1988 exhibit some degree of phason strain (Horn *et al.*, 1986; Heiney *et al.*, 1987).

Finally, in Fig. 8(c) we illustrate a “faceted” acceptance domain that produces a real-space structure that is not aperiodic, but consists of a set of microcrystalline approximants to the aperiodic structure. It is particularly illuminating to compare Figs. 8(b) and 8(c), since one can anticipate increasing difficulty in discriminating between phason-strained quasicrystals and such microcrystalline approximants as the order of the approximant increases.

A careful examination of many apparently quasicrystalline diffraction patterns reveals spot shifting and spot anisotropy; further, low-intensity peaks frequently develop in the diffraction patterns of annealed quasicrystals. While these effects are often explained in terms of phason strain, they can also be characteristic of high-order rational crystalline approximants. These two approaches

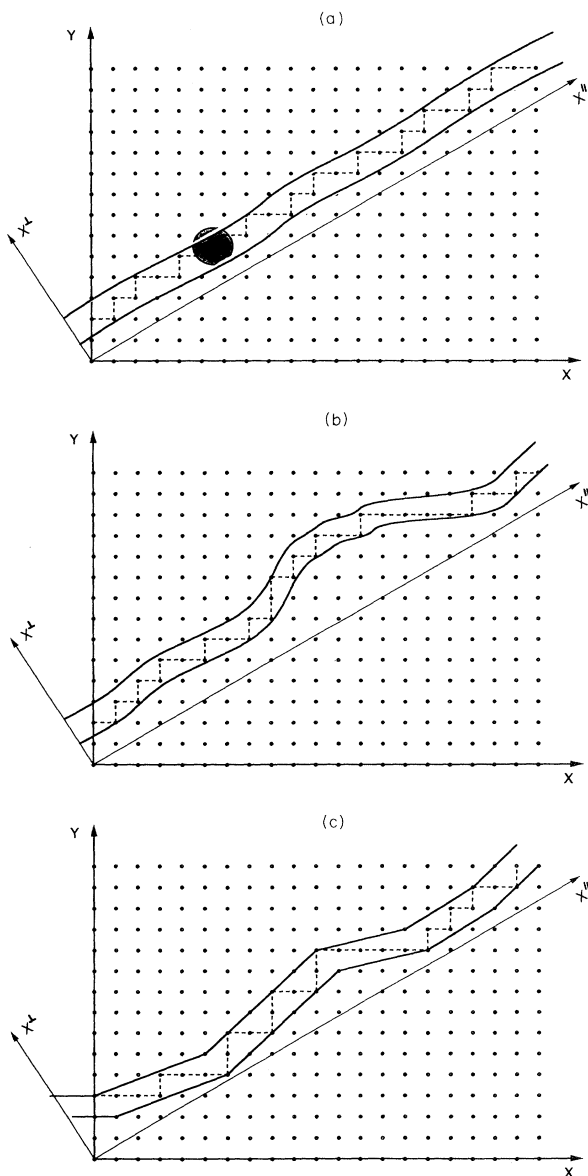


FIG. 8. Schematic of other possible structures for quasicrystals using the cut and project method. (a) A meandering, but bounded, acceptance volume produces a structure which, on average, is a Fibonacci sequence with some defects (random-tiling models). One defect is found in the shaded circle [compare with Fig. 6(b)]. (b) A meandering, unbounded acceptance volume produces a heavily disordered sequence (icosahedral-glass or phason-strained quasicrystal). (c) A faceted acceptance domain, with commensurate slopes, can produce regions of microcrystalline approximants.

are in many ways equivalent; arguments favoring one or the other often enter the realm of philosophy.

## B. Quasicrystals and approximants in two and three dimensions

Extending the discussion in Sec. II.A to higher dimensions is straightforward but difficult to visualize. Imagine starting with a periodic lattice of points in five dimensions. If a two-dimensional plane representing the two-dimensional physical space is oriented perpendicular to the body diagonal of the five-dimensional cube, the cube edges will project onto five line segments of the same length, equally spaced around a circle. The resulting full projection is actually a 2D Penrose tiling, which produces a pattern of Bragg diffraction spots that reflects the symmetry of the 5D lattice. In particular, the body diagonal of the five-dimensional cube is a fivefold symmetry axis, just as the body diagonal of a three-dimensional cube is a threefold axis. Consequently, the diffraction pattern also has fivefold symmetry.

For the icosahedral alloys, characterized by six fivefold axes, the 3D structure results from the projection of points of a 6D hypercubic lattice that are contained in a 3D acceptance domain appropriately oriented (see below) with respect to the 6D lattice. The analog of the acceptance strip of width  $L$  in the  $X^\perp$  direction for the 2D to 1D projection is a triacontahedron in the 3D space ( $X^\perp$ ) orthogonal to the physical space ( $X^\parallel$ ). The analogs of the  $l$  and  $s$  segments that result from the projection of points in the acceptance strip for the 2D to 1D projection are oblate and prolate rhombohedra. The edge length of these rhombohedra  $a_R$ , plays a role analogous to the lattice constant for periodic crystals and is therefore called the *quasilattice constant* for the tiling (Elser, 1985a).<sup>8</sup>

As discussed in Sec. III.A, rational crystalline approximants can be constructed by generalizing the projection scheme (Elser and Henley, 1985; Kulkarni, 1989; Torres *et al.*, 1989; Mukhopadhyay *et al.*, 1991). Changing the orientation of the acceptance domain with respect to the 6D hypercubic lattice yields a large cubic unit-cell crystalline phase that approximates locally the structure of the icosahedral phase. For the icosahedral phase, the orientations of the acceptance domain and the physical space are specified by a  $6 \times 6$  orientation matrix given by

$$M = \frac{1}{(2\tau^3 + 2)^{1/2}} \begin{pmatrix} 1 & -1 & 0 & \tau & \tau & 0 \\ \tau & \tau & 1 & 0 & 0 & 1 \\ 0 & 0 & \tau & 1 & -1 & -\tau \\ -\tau & \tau & 0 & 1 & 1 & 0 \\ 1 & 1 & -\tau & 0 & 0 & -\tau \\ 0 & 0 & 1 & -\tau & \tau & 1 \end{pmatrix} = \begin{pmatrix} \mathbf{X}^\parallel \\ \mathbf{X}^\perp \end{pmatrix}. \quad (3)$$

<sup>8</sup>The scaling constant  $g_0$  introduced in the indexing scheme described in Sec. III.A is given by  $\pi/a_R$ .

The upper three row vectors give the 6D coordinates of three vectors that span the physical space ( $\mathbf{X}^{\parallel}$ ), and the lower three rows are the vectors spanning the orthogonal space ( $\mathbf{X}^{\perp}$ ). The columns of  $\mathbf{X}^{\parallel}$  and  $\mathbf{X}^{\perp}$  give the 3D coordinates of the 6D basis vectors in the physical and orthogonal subspaces, respectively.

A cubic rational approximant is obtained when  $\tau$ , in the lower three rows of the orientation matrix, is replaced by an integer ratio  $q/p$  that approximates  $\tau$ . A particular set of crystalline approximants, the Fibonacci rational approximants, are obtained if  $q$  and  $p$  are replaced by two consecutive members of the Fibonacci series:

$$q/p: 1/1, 2/1, 3/2, 5/3, 8/5, 13/8, \\ 21/13, 34/21, \dots$$

We emphasize that the rational ratio is not restricted to the Fibonacci series, since non-Fibonacci rational approximants have been observed experimentally (see Sec. III.C).

Elser and Henley (1985) first demonstrated that the cubic  $\alpha(\text{AlMnSi})$  and Bergman structures can be obtained by a 1/1 rational projection from the same atomic decoration of the 6D hypercubic lattice used to define the icosahedral phases. They also made the first quantitative assessment of the similarities between these bcc [or almost bcc in the case of  $\alpha(\text{AlMnSi})$ ] phases and the structure of the icosahedral phase, demonstrating that the atomic structures of the crystal phases can be constructed from the same building blocks assumed for the icosahedral phases. These building blocks may be taken either as the icosahedral clusters of atoms described in Sec. II.B, or as a set of two types of rhombohedral bricks, described above, which may also be derived from the decomposition of the icosahedral clusters.

Henley (1986) argued that icosahedral alloys can be classified, based on structural differences in their crystalline approximants, by the ratio of their *quasilattice constant*  $a_R$  to the typical interatomic spacings  $d$  determined from the appropriate approximant. If  $a_R/d \approx 2.0$ , the  $i$ -phase belongs to the (Al,Zn)Mg class; if  $a_R/d \approx 1.65$ , it belongs to the (AlMnSi) class. Using this method, most quasicrystals appear to fall into the (AlMnSi) class, including  $i(\text{PdUSi})$ ,  $i(\text{AlCuV})$ ,  $i(\text{TiMnSi})$ , and  $i(\text{AlCuFe})$ ;  $i(\text{AlLiCu})$  belongs to the (Al,Zn)Mg class. A similar classification scheme has been proposed by Yang (1988).

The lattice parameters of approximants increase with the order of the rational approximant; they are determined readily by projecting the 6D vectors that define the edges of the 3D unit cells using the orientation matrix for the approximant. For a cubic 6D lattice and integers  $p$  and  $q$ ,

$$a_{q/p} = \frac{2(p + q\tau)a_R}{(2 + \tau)^{1/2}}, \tag{4}$$

where, again,  $a_R$  is the quasilattice constant defined as the edge length of the rhombohedral cells constituting

the 3D Penrose lattice or, equivalently, the projection of the basis vectors of the 6D hypercubic lattice onto the 3D physical space.

To emphasize the correspondence between the diffraction patterns from crystalline approximants and the icosahedral phase, the prominent reflections for the crystalline approximants can be written in terms of a set of distorted basis vectors [see Eq. (1)],  $\hat{\mathbf{e}}_{i,q/p}$  as

$$\mathbf{G}_{q/p}^{\parallel} = \frac{\pi}{a_{q/p}} \sum_{i=1}^6 n_i \hat{\mathbf{e}}_{i,q/p}^{\parallel}, \tag{5}$$

$$\hat{\mathbf{e}}_{i,q/p}^{\parallel} = \frac{1}{(p^2 + q^2)^{1/2}} \begin{bmatrix} p & q & 0 \\ -p & q & 0 \\ 0 & p & q \\ q & 0 & p \\ q & 0 & -p \\ 0 & p & -q \end{bmatrix} \begin{bmatrix} i \\ j \\ k \end{bmatrix}.$$

These basis vectors point to the vertices of a distorted icosahedron. For the undecorated lattice, the diffraction pattern can be calculated in a manner analogous to the prescription in Sec. II.A for the acceptance strip used for the 2D to 1D projection. The intensities of the diffraction spots are determined by the Fourier transform of the acceptance domain.

Figure 9 shows calculated diffraction patterns taken along the pseudo-fivefold direction for different values of  $q/p$ . The size of the spots corresponds directly with their intensities, taken to be inversely proportional to the

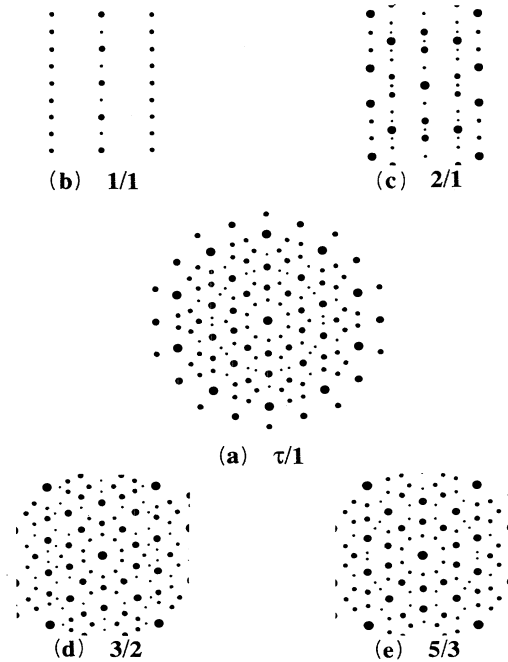


FIG. 9. Calculated diffraction patterns along the fivefold axis for successive Fibonacci approximants to the icosahedral phase: (a)  $q/p = \tau/1$ , a "perfect" quasicrystal; (b)  $q/p = 1/1$ ; (c)  $q/p = 2/1$ ; (d)  $q/p = 3/2$ ; (e)  $q/p = 5/3$ .

values of  $G_{q/p}^{\perp}$ . For comparison, the fivefold diffraction pattern calculated for the icosahedral phase is also shown. Diffraction patterns from the lower-order approximants, such as the 1/1 and 2/1, clearly display the periodicity of the Bravais lattice; they are distinct from the patterns of the  $i$ -phase. As the order of the approximant increases, however, this distinction becomes less clear. The 3/2 approximant is distinguishable from the icosahedral phase by the elongation of the inner circle of

spots in the pseudo-fivefold pattern and the distortions of the small pentagonal arrangements of spots. The pseudo-fivefold diffraction pattern from the 5/3 approximant in Fig. 9 is nearly indistinguishable from the fivefold pattern of the icosahedral quasicrystal.

A more quantitative assessment of the shifts in diffraction spot positions between a quasicrystal and its rational approximant has been described in detail by Mukhopadhyay *et al.* (1991). Denoting the reciprocal-

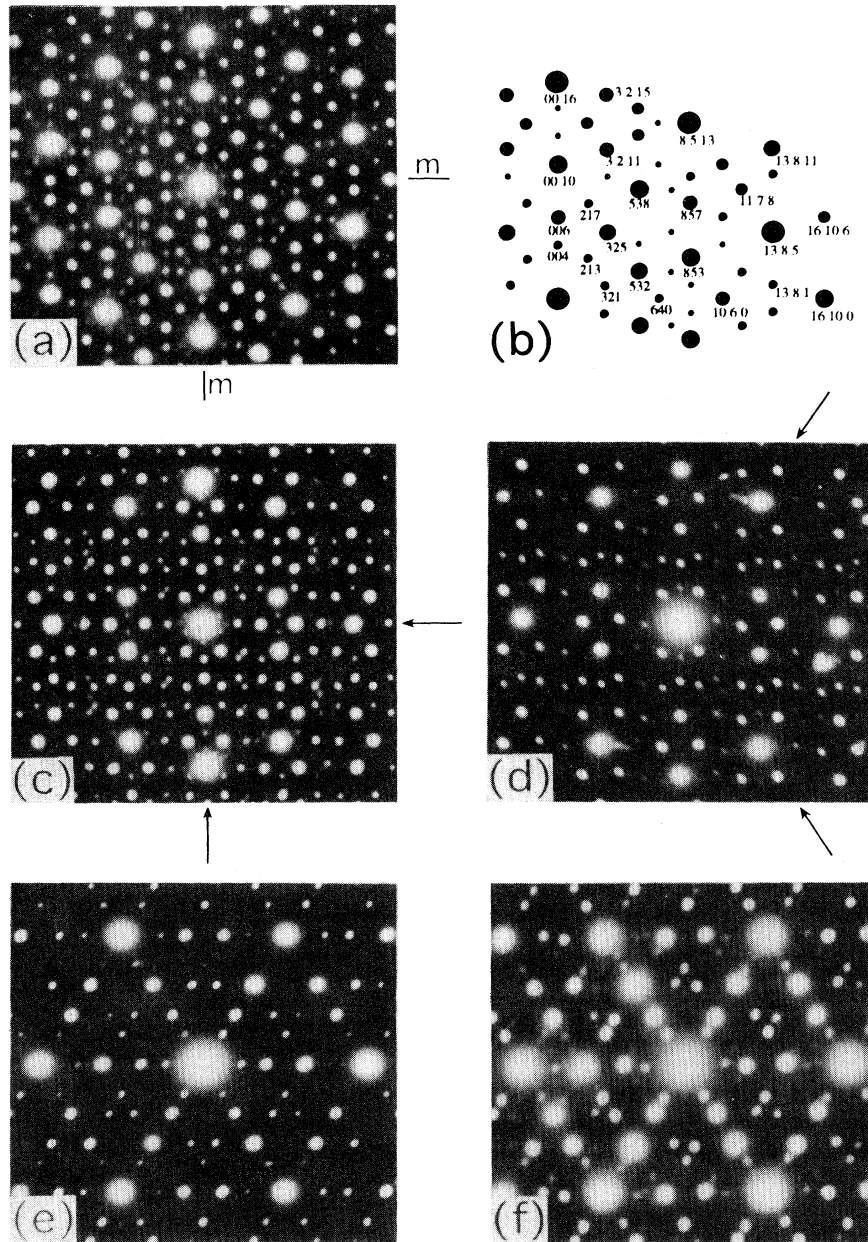


FIG. 10. Experimental selected area diffraction (SAD) patterns in  $\text{Ti}_{54}\text{Zr}_{26}\text{Ni}_{20}$ : (a) along the pseudo-fivefold axis; (b) an indexing of the pattern in (a) using cubic indices; (c) twofold axis along  $[100]$ ; (d) pseudo-twofold axes along other icosahedrally equivalent directions; (e) threefold axis along  $[111]$  of the cubic unit cell; (f) pseudo-threefold axes along other icosahedrally equivalent directions (from Zhang and Kelton, 1992).

lattice vector of a reflection from the icosahedral phase by  $\mathbf{G}_I^\parallel$ , and that from the rational approximant by  $\mathbf{G}_{q/p}^\parallel$ , they show that

$$\Delta\mathbf{G} = \mathbf{G}_I^\parallel - \mathbf{G}_{q/p}^\parallel = \frac{\tau - pq}{1 + (q/p)\tau} \mathbf{G}_I^\perp. \quad (6)$$

From Eq. (6) one sees that  $\Delta\mathbf{G} \rightarrow 0$  as the ratio  $q/p \rightarrow \tau$ , and that the magnitude and direction of the displacement depends upon the  $\mathbf{G}^\perp$  of the icosahedral peak; peaks with larger  $\mathbf{G}^\perp$  values are shifted more. Quite frequently, the diffraction peaks from crystalline approximants appear to be asymmetric distortions of the icosahedral peaks in TEM patterns, similar to the effect of phason strain. In order to distinguish clearly between the two patterns, high-resolution x-ray-diffraction measurements of the peak positions are required.

### C. Observed rational approximants

Subsequent to the first observation that  $\alpha(\text{AlMnSi})$  and the Bergman  $(\text{Al,Zn})\text{Mg}$  crystal structures could be obtained by a 1/1 rational projection, similar phases have been identified in a wide variety of alloys, including Ti-Fe-Si (Dong *et al.*, 1987), Ti-Mn-Si (Holzer *et al.*, 1989), TiCrSi (Libbert *et al.*, 1992), Ti-V-Si (Zhang and Kelton, 1991), Ga-Mg-Zn (Spaepen *et al.*, 1990), Al-Li-Cu (Marcus and Elser, 1986), and Al-Cu-Ru (Shield *et al.*, 1992).

The 2/1 cubic approximant reported in Ga-Mg-Zn, shown in Fig. 11(c), was reported by Spaepen *et al.* (1990). 3/2 cubic approximants have also been observed, first in Mg-Al-Zn (Mukhopadhyay *et al.*, 1991) and more recently in Ti-Zr-Ni alloys (Zhang and Kelton, 1992), giving identical diffraction patterns in both cases. The diffraction patterns for 3/2 (Ti-Zr-Ni) are shown in Fig. 10. Despite their similarity to the diffraction patterns from the *i*-phase, they clearly have a lower symmetry. The fivefold symmetry [Fig. 10(a)], for example, has been reduced to a twofold symmetry due to small shifts in the spot positions. The first circle of spots around the center has been distorted into an ellipse [in agreement with the 3/2 calculated pseudo-fivefold pattern shown in Fig. 9(d)]. Similar distortions are also evident in the twofold and threefold patterns. Because of the lower cubic symmetry, only eight of the 20 icosahedral threefold zones can be aligned parallel to cubic  $\langle 111 \rangle$  directions; only six of the icosahedral twofold zones are then parallel to cubic  $\langle 100 \rangle$  directions. There are therefore two inequivalent pseudo-icosahedral twofold zones [Figs. 10(c) and 10(d)]. Those patterns taken along the  $\langle 100 \rangle$  directions show the spots shifted along twofold directions; spots are shifted along fivefold directions in the other patterns. Similarly, threefold patterns lying along the cubic  $\langle 111 \rangle$  directions have true threefold rotational symmetry; those lying along the other directions have only a twofold symmetry [Figs. 10(e) and 10(f)]. All of these patterns can be indexed to a cubic structure; this is demonstrated in Fig. 11(b) for one quadrant of the

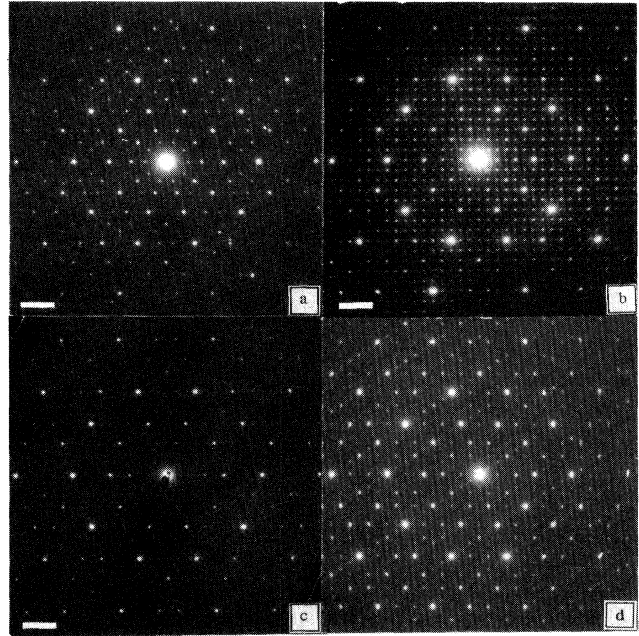


FIG. 11. Icosahedral fivefold and pseudo-fivefold diffraction patterns of the *i*-phase and three crystalline approximants in Ga-Mg-Zn: (a) *i*-phase; (b) 3/2-2/1-2/1 side-centered orthorhombic phase along the [110] zone axis; (c) 2/1 cubic phase along the [058] zone axis; (d) 2/1 rhombohedral phase along the [001] zone axis. The marker in the figure corresponds to  $1 \text{ \AA}^{-1}$  (from Spaepen *et al.*, 1990).

pseudo-fivefold pattern.

As already mentioned, the ratio of integers that define the approximant need not be members of the Fibonacci series. Other cubic rational approximants have been reported in Al-W-Fe by, for example, Mukhopadhyay *et al.* (1992). The concept of rational approximants can be generalized even further to include projections from noncubic 6D lattices, such as tetragonal, orthorhombic, and rhombohedral. Spaepen *et al.* (1990) have identified 3/2-2/1-2/1 side-centered orthorhombic and 2/1 rhombohedral approximants in conventionally solidified GaMgZn alloys, shown in Fig. 11. Hexagonal, orthorhombic, and 1/1 cubic lattices have been reported in annealed Ti-Mn-Si alloys, resulting from a transformation of the *i*-phase in the quenched samples. From TEM studies, those titanium transition-metal phases appear to be constructed from identical icosahedral units packed in different arrangements (Levine *et al.*, 1992).

Although we have not discussed the quasicrystallography of other aperiodic structures, we point out that crystalline approximants to other quasicrystals also exist. The most impressive example forms in slowly cooled Al-Cu-Co alloys as an approximant to the decagonal phase, a quasicrystal that is periodic in one dimension and quasiperiodic in the other two. Figure 12 shows an enlarged view of one quadrant from a pseudo-tenfold pattern of this approximant, where the intensity modula-

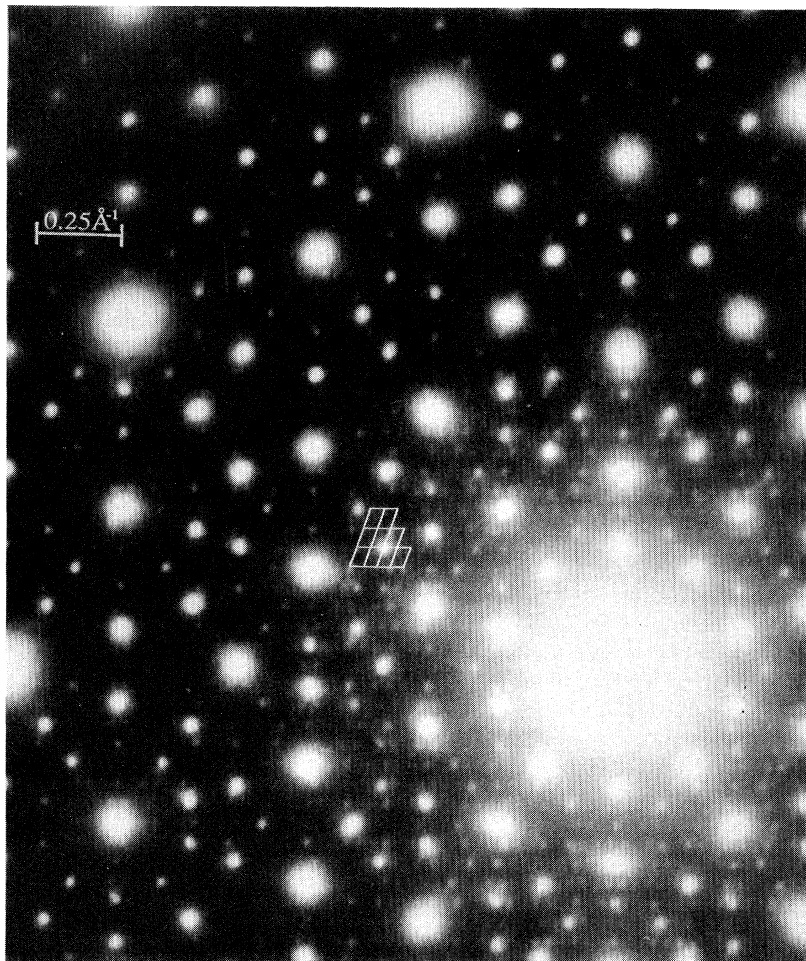


FIG. 12. Magnified region of a portion of the pseudo-tenfold selected area diffraction (SAD) pattern from decagonal  $\text{Al}_{64}\text{Co}_{22}\text{Cu}_{14}$  showing the periodic array of diffraction spots, corresponding to a repeat distance of about 100 Å (from Daulton and Kelton, 1992).

tions give rise to a striking, nearly tenfold pattern. Closer inspection, however, reveals a rhombic array of finely spaced periodic diffraction spots (indicated in white), with a spacing that corresponds to a unit-cell dimension of over 100 Å (Daulton *et al.*, 1992). Earlier indications of this phase were found in bright-field TEM photographs (Launois *et al.*, 1990). While the existence of intermetallic crystalline phases with unit-cell edge lengths between 50 and 100 Å was undreamed of only a few years ago, they now appear to be quite common, especially in aluminum and titanium transition-metal alloys.

#### IV. USING CRYSTALLINE APPROXIMANTS TO MODEL THE STRUCTURE OF QUASICRYSTALS

Having established the close structural relationships between icosahedral quasicrystals and their respective approximants, we now briefly describe some of the

methods employed to model quasicrystalline structures using the known structure of the crystalline approximants. Structural units, such as the Mackay icosahedra or prolate and oblate rhombohedra, are assumed to be the fundamental units in quasicrystals and crystal approximants. The decorations of these clusters are determined by fitting x-ray-diffraction patterns taken from the crystalline phases. Following the methods of standard crystallography, the atomic structures of quasicrystals are defined by constructing a tiling network (somewhat equivalent to a Bravais lattice) and decorating that network with the clusters. Two tiling/cluster-based approaches are popular. The first approach is based upon the aperiodic packings of two inequivalent tiles. There are two equilibrium binary tiling models that employ oblate and prolate rhombohedra that have been mentioned in Sec. III.A. Penrose tiling models minimize the enthalpic contribution to the free energy by imposing rigid matching rules for the tiling. The random-tiling models minimize the free energy by maximizing the entropic contribution at nonzero temperature. Which tiling pro-

vides the more appropriate description of quasicrystalline structures is still a matter of debate.

An alternative, nonequilibrium tiling- or cluster-based approach is indicated by the considerable evidence for the existence of icosahedral clusters in undercooled liquids and glasses, as well as in the crystalline approximants. If a liquid were cooled sufficiently fast, these clusters would have insufficient time to pack into the periodic arrangement of the approximants. Instead, they may pack with the correct local symmetry but with reduced coordination number, forming an orientationally ordered but translationally disordered random-cluster packing, first called the icosahedral glass. For some icosahedral phases (especially the titanium-based quasicrystals), the icosahedral glass model is likely a good one. Interestingly, Henley (1991) has argued that, as the environmental constraints are increased further, a random tiling results, suggesting a continuum of possible atomic structures for quasicrystals. Following the methods for the binary tilings, the atomic decoration of such structures is obtained by identifying fundamental clusters within the crystal approximants and assuming that their integrity is maintained with different packings.

Finally, an alternate approach employing the cut and project method, described in Sec. III, uses the atomic decoration of clusters found in the approximant phases to define the atomic basis of the 6D hypercubic lattice. The quasicrystalline structure in 3D is then determined by reorienting the acceptance domain and projecting the structure back into three dimensions. Taking  $\alpha(\text{AlMnSi})$  to be a 1/1 projection, Cahn *et al.* (1988a, 1988b) and Gratias *et al.* (1988) determined the atomic decoration of the hypercubic lattice from a Patterson map constructed from scattering studies of that phase. Using that decoration and changing the window orientation to that for the quasicrystal, the atomic structure of  $i(\text{AlMnSi})$  was obtained. Although reasonable agreement with measured diffraction intensities was demonstrated, the resultant structure contained many unphysically short atomic separations. The proper choice of polyhedral atomic surfaces in 6D, instead of the spherical ones first assumed, avoids many of these problems, giving reasonable atomic distances, the correct density, and a local structure similar to that of  $\alpha(\text{AlMnSi})$ , containing a large number of Mackay icosahedra (MI) (66.6% of the atoms reside in MIs as opposed to 78.3% in the  $\alpha$  phase). This method and its refinements (see, for example, Qiu and Jaric, 1990) have also been applied to the structural determination of several quasicrystalline systems. Presently, this seems to be the best technique available for determining the local atomic structure of the icosahedral phase in something approaching an unambiguous manner.

## V. PHASE TRANSITIONS BETWEEN APPROXIMANTS AND QUASICRYSTALS

It has been suggested that upon annealing, some quasicrystals crystallize by transforming through a succession

of rational approximants (see, for example, Chattopadhyay and Mukhopadhyay, 1987; Zhang and Kuo, 1990). As discussed in Sec. III.A, long-wavelength phason fluctuations in quasicrystals modify the local atomic configurations. These can lock into special values to produce periodic approximants to the quasicrystal. All possible phason-induced structural modifications expected for the icosahedral phase were recently enumerated by Ishii (1989). These include space-group modifications resulting in the approximants discussed above.

Transmission electron microscope investigations of  $i(\text{AlCuFe})$  (Audier and Guyot, 1990) provide the best evidence for a reversible structural transformation to a lower-symmetry crystalline phase at 670 °C. The x-ray-scattering intensity of the high  $|\mathbf{G}^\perp|$  peaks increases dramatically with annealing, suggesting a soft-phason mechanism analogous to the more familiar phonon softening mode for some phase transformations in crystalline structures. Transmission electron microscope studies show an increased spot anisotropy below the transition temperature [Fig. 13(a)] that can be explained as a transformation to a fine-grained rhombohedral approximant phase. As illustrated by a comparison of Figs. 13(a) and 13(b), the twinned periodic structure below the transition temperature ( $T_c$ ) can be distinguished from the

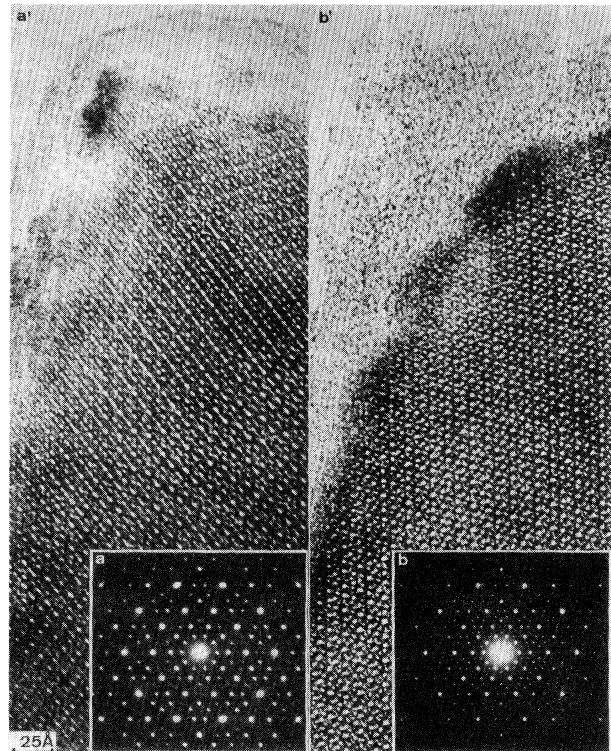


FIG. 13. Comparison of the electron diffraction patterns and high-resolution micrographs of the same area of an Al-Cu-Fe sample: (a) crystalline rhombohedral phase below 670 °C; (b) icosahedral quasicrystal above 670 °C (from Audier and Guyot, 1990).

icosahedral structure above  $T_c$  in the TEM and high-resolution electron microscopy (HREM) images.

## VI. ELECTRONIC AND ELECTRON-TRANSPORT PROPERTIES OF QUASICRYSTALS AND APPROXIMANTS

Initial studies of electron transport in the icosahedral phase indicated metallic glasslike behavior, with large residual resistivities ( $\rho_0$  of order  $100 \mu\Omega \text{ cm}$ ) and small negative temperature coefficients, presumably reflecting the structural disorder indicated by peak broadening in x-ray-diffraction patterns (Berger *et al.*, 1986; Kelton and Holzer, 1988). In more recent studies of Al-Cu-Fe and Al-Cu-Ru alloys, however, in which stable, virtually defect-free icosahedral phases can be formed, the resistivity is enormous, increasing to over  $10\,000 \mu\Omega \text{ cm}$  as the degree of structural order increases (Biggs *et al.*, 1990; Mizutani *et al.*, 1990; Klein *et al.*, 1991). Never before have such large resistivities, approaching the minimum metallic conductivity (Mott, 1987), been reported in good metal alloys. Furthermore, the resistivity decreases at high temperature, reminiscent of what is observed in heavily doped semiconductors. Anomalies have been observed in other probes of transport properties, including the Hall effect, thermopower, and in the low-temperature specific heat (see Poon, 1992). All of these features suggest the presence of a gap (or pseudogap) in the electronic density of states near the Fermi energy.

Do these unusual transport properties arise by scattering from the quasilattice, or do they result from the local icosahedral structural order common to the *i*-phase and crystalline approximants? Annealed (and hence well-ordered) samples of  $\alpha(\text{AlMnSi})$  have high room-temperature and residual resistivities [ $\rho(300 \text{ K}) \approx 3100 \mu\Omega \text{ cm}$  with  $\rho(0.5 \text{ K})/\rho(300 \text{ K}) \approx 2$ ], and large low-temperature Hall ( $R_H$ ) and thermoelectric power ( $S$ ) coefficients with anomalous temperature dependences (Poon, 1992). Small values for the low-temperature specific heat ( $\gamma = 0.6 \text{ mJ/g-at. K}$ ) indicates a low density of carriers. Similar features are also found in rhombohedral Al-Cu-Fe, corresponding well with those found in the *i*-phase.

Questions of electronic structure are typically centered around questions of formation and stability. The fundamental question remains unanswered: Why is icosahedral order so strongly preferred in many cases? The answer, of course, must come from considerations of atomic size, strain, and kinetic and electronic effects. One approach (Villars *et al.*, 1986; Rabe *et al.*, 1992), based on the isolation of certain structures to regions of multidimensional diagrams of phenomenological variables constructed from electronegativity data, atomic valences, atomic sizes, etc., has proved useful although it is not clear that this method is more predictive than considerations of similar crystalline structures, for example.

A more fundamental approach is the study of the stability of local atomic configurations. Since Bloch's

theorem is inapplicable for quasicrystals, interferences must be drawn from calculations on small clusters and crystal approximants. Fujiwara (1989) first calculated the electronic density of states (DOS) for  $\alpha(\text{AlMnSi})$ ; similar calculations have also been made for  $R(\text{AlLiCu})$ ,  $\text{AlMgZn}$ , and the decagonal approximant  $\text{Al}_{13}\text{Fe}_4$ . These show that the Mackay icosahedron and the truncated icosahedron, present in the 1/1 approximants and presumably present in the higher-order rational approximants, and the icosahedral phase are particularly stable units, supporting their use in structural models.

While Brillouin zones, as such, cannot be constructed for aperiodic crystals, some experimental and theoretical studies of electronic and vibrational properties of the icosahedral phase indicate the existence of "quasizones" (Benoit *et al.*, 1990; Niizeki and Akamatsu, 1990; Goldman *et al.*, 1992; Poon, 1992). A Hume-Rothery mechanism, where a pseudogap develops in the DOS (arising from the Fermi surface touching the quasi-Brillouin-zone boundary), increases the cohesive energy and may then stabilize the crystalline or quasicrystalline structures. This works most efficiently in icosahedral quasicrystals, because the quasizones are almost spherical. The high resistivities observed are consistent with the Hume-Rothery mechanism. The unusual behavior of  $S(T)$  and  $R_H$  and the dramatic changes in these quantities and in  $\rho(T)$  with small (near 1 at. %) compositional variations in  $i(\text{AlCuRu})$ ,  $i(\text{AlCuFe})$ , and  $i(\text{AlCuRuSi})$  also suggest a low concentration of carriers at  $E_F$ . In addition, soft-x-ray spectroscopy studies in quasicrystals and high-order approximants indicate the presence of a deep minimum in the DOS; the pseudogap is wider and deeper in the quasicrystal than in the approximant (Belin and Danhkaizi, 1992).

As well as providing a means for understanding quasicrystal and crystal approximant formation, these observations suggest that the unusual transport properties, including the tendency toward a metal-insulator transition, do not arise from scattering effects of the quasilattice, but result from a reduction in the carrier concentration caused by the opening of the pseudogap in systems with local icosahedral order. It appears that electronic and transport properties unique to the quasicrystal arising solely from its quasiperiodicity have yet to be discovered. These points are discussed in more detail in the several review articles written recently on these subjects (Carlsson and Phillips, 1991; Fujiwara and Tsunetsuga, 1991; Kimura and Takeuchi, 1991; Poon, 1992).

## VII. CONCLUDING REMARKS

In the seven years of intense study since their discovery, quasicrystals have evolved from their initial position as a laboratory curiosity to, perhaps, the most thoroughly studied class of intermetallic compounds. In fact, instead of forming rarely under only highly idealized conditions, quasicrystals occur frequently. In many ways, however, the field of research has come full circle.

In 1985, most researchers in the field found themselves defending the very existence of quasicrystals against the position that they were merely large unit-cell, possibly twinned crystals. Now, many of those same researchers have turned to the study of complex crystalline structures, so closely similar to quasicrystals that only extremely precise measurements can distinguish the two structures, in order to gain additional insight into the structure, properties, and formability of the quasicrystalline phase.

These crystalline approximants have provided a wealth of information on such questions, serving as good starting points for structural determinations and calculated vibrational and electronic structures for quasicrystals. Due to their large unit-cell sizes, however, even these calculations are more difficult than those usually attempted and will require new techniques and insight for their solution. Such studies must be fueled by experimental measurements of the electrical, structural, and mechanical properties of both crystalline and quasicrystalline alloys. Clearly, this field is still in its infancy; exciting discoveries and further insights into the rules employed by nature to form condensed-matter phases are yet ahead.

#### ACKNOWLEDGMENTS

The authors wish to acknowledge the very useful comments and suggestions of P. C. Gibbons, S. Ranganathan, and N. K. Mukhopadhyay. Ames Laboratory is operated for the U.S. Department of Energy by Iowa State University under Contract No. W7405-ENG-82. Work at Washington University was partially supported by the National Science Foundation under Contract No. DMR-89-03081.

#### REFERENCES

- Amelinckx, S., C. Van Heurck, and G. Van Tendeloo, 1990, in *Quasicrystals and Incommensurate Structures in Condensed Matter*, edited by M. J. Yacaman, D. Romeu, V. Castano, and A. Gomez (World Scientific, Singapore), p. 300.
- Audier, M., Y. Bréchet, M. de Boissieu, P. Guyot, C. Janot, and J. M. Dubois, 1991, *Philos. Mag. B* **63**, 1375.
- Audier, M., and P. Guyot, 1990, in *Quasicrystals*, edited by M. V. Jaric and S. Lundqvist (World Scientific, Singapore), p. 74.
- Audier, M., P. Sainfort, and B. Dubost, 1986, *Philos. Mag. B* **54**, L105.
- Bak, P., 1985a, *Phys. Rev. Lett.* **54**, 1517.
- Bak, P., 1985b, *Phys. Rev. B* **32**, 5764.
- Ball, M. D., and D. J. Lloyd, 1985, *Scr. Metall.* **19**, 1065.
- Bancel, P. A., 1989, *Phys. Rev. Lett.* **63**, 2741.
- Bancel, P. A., P. Heiney, P. W. Stephens, A. I. Goldman, and P. M. Horn, 1985, *Phys. Rev. Lett.* **54**, 2422.
- Belin, E., and Z. Danhkzai, 1992, *J. Non-Cryst. Solids*, in press.
- Bendersky, L., 1985, *Phys. Rev. Lett.* **55**, 1461.
- Benoit, C., G. Poussigue, and A. Azougarh, 1990, *J. Phys. Condens. Matter* **2**, 2519.
- Berger, C., D. Pavuna, and F. Cyrot-Lackmann, 1986, *J. Phys. (Paris) Colloq.* **47**, C3-489.
- Bergman, G., J. L. T. Waugh, and L. Pauling, 1957, *Acta Crystallogr.* **10**, 254.
- Biggs, B. D., S. J. Poon, and N. R. Munirathnam, 1990, *Phys. Rev. Lett.* **65**, 2700.
- Cahn, J. W., D. Gratias, and B. Mozer, 1988a, *J. Phys. (Paris)* **49**, 1225; Cahn, J. W., D. Gratias, and B. Mozer, 1988b, *Phys. Rev. B* **38**, 1638.
- Cahn, J. W., D. Shechtman, and D. Gratias, 1986, *J. Mater. Res.* **1**, 13.
- Carlsson, A. E., and R. Phillips, 1991, in *Quasicrystals: The State of the Art*, edited by D. P. DiVincenzo and P. J. Steinhardt (World Scientific, Singapore), p. 361.
- Chattopadhyay, K. S. Lele, S. Ranganathan, G. N. Subbanna, and N. Thangaraj, 1985, *Curr. Sci.* **548**, 895.
- Chattopadhyay, K., and N. K. Mukhopadhyay, 1987, *Mater. Sci. Forum* **22-24**, 639.
- Chattopadhyay, S., S. Lele, N. Thangaraj, and S. Ranganathan, 1987, *Acta Metall. Mater.* **35**, 727.
- Chen, C. H., and H. S. Chen, 1986, *Phys. Rev. B* **33**, 2814.
- Chen, H. S., and A. Inoue, 1987, *Scr. Metall.* **22**, 527.
- Chen, H., D. X. Li, and K. H. Kuo, 1988, *Phys. Rev. Lett.* **60**, 1645.
- Cherkashin, E. E., P. I. Kripyakevich, and G. I. Oleksiv, 1963, *Kristallografiya* **8**, 846 [*Sov. Phys. Crystallogr.* **8**, 681 (1964)].
- Cooper, M., and K. Robinson, 1966, *Acta Crystallogr.* **20**, 614.
- Daulton, T. L., and K. F. Kelton, 1992, *Philos. Mag. B* **66**, 37.
- Daulton, T. L., K. F. Kelton, S. Song, and E. Ryba, 1992, *Philos. Mag. Lett. B* **65**, 55.
- deBruijn, N. G., 1981, *Proc. K. Ned. Akad. Wet. A* **84**, 39.
- de Wolff, P. M., 1974, *Acta Crystallogr. A* **30**, 777.
- DiVincenzo, D. P., and P. J. Steinhardt, 1991, Eds., *Quasicrystals: The State of the Art* (World Scientific, Singapore).
- Dong, C., K. Chattopadhyay, and K. H. Kuo, 1987, *Scr. Metall.* **21**, 1307.
- Duneau, M., and A. Katz, 1985, *Phys. Rev. Lett.* **54**, 2688.
- Elser, V., 1985a, *Phys. Rev. B* **32**, 4892.
- Elser, V., 1985b, *Phys. Rev. Lett.* **54**, 1730.
- Elser, V., 1986, *Phys. Rev. B* **32**, 4892.
- Elser, V., 1987, in *Proceedings of the XVth International Colloquium on Group Theoretical Methods in Physics*, edited by R. Gilmore and D. H. Feng (World Scientific, Singapore).
- Elser, V., and C. L. Henley, 1985, *Phys. Rev. Lett.* **55**, 2883.
- Frank, F. C., and J. S. Kasper, 1958, *Acta Crystallogr.* **11**, 184.
- Frank, F. C., and J. S. Kasper, 1959, *Acta Crystallogr.* **12**, 483.
- Fujiwara, T., 1989, *Phys. Rev. B* **40**, 942.
- Fujiwara, T., and Tsunetsuga, 1991, in *Quasicrystals: The State of the Art*, edited by D. P. DiVincenzo and P. J. Steinhardt (World Scientific, Singapore), p. 343.
- Goldman, A. I., C. Stassis, M. deBoissieu, R. Currat, C. Janot, R. Bellissent, H. Moudden, and F. W. Gayle, 1992, *Phys. Rev. B* **45**, 10280.
- Goldman, A. I., and M. Widom, 1991, *Annu. Rev. Phys. Chem.* **42**, 685.
- Gratias, D., J. W. Cahn, and B. Mozer, 1988, *Phys. Rev. B* **38**, 1643.
- Guryan, C. A., A. I. Goldman, P. W. Stephens, K. Hiraga, A. P. Tsai, A. Inoue, and T. Masumoto, 1989, *Phys. Rev. Lett.* **62**, 2409.
- Guryan, C. A., P. W. Stephens, A. I. Goldman, and F. W. Gayle, 1988, *Phys. Rev. B* **37**, 8495.
- Guyot, P., P. Kramer, and M. de Boissieu, 1991, *Rep. Prog. Phys.* **54**, 1373.

- He, L. X., X. Z. Li, Z. Zhang, and K. H. Kuo, 1988, *Phys. Rev. Lett.* **61**, 1116.
- Heiney, P. A., P. A. Bancel, P. M. Horn, J. L. Jordan, S. LaPlaca, J. Angilello, and F. W. Gayle, 1987, *Science* **238**, 660.
- Henley, C. L., 1986, *Philos. Mag.* **B 53**, L59.
- Henley, C. L., 1988, *J. Phys. A* **21**, 1649.
- Henley, C. L., 1991, in *Quasicrystals: The State of the Art*, edited by D. P. DiVincenzo and P. J. Steinhardt (World Scientific, Singapore), p. 429.
- Holzer, J. C., K. F. Kelton, L. E. Levine, and P. C. Gibbons, 1989, *Scr. Metall.* **23**, 691.
- Horn, P. M., W. Malzfeldt, D. DiVincenzo, J. Toner, and R. Gambino, 1986, *Phys. Rev. Lett.* **57**, 1444.
- Ishii, Y., 1989, *Phys. Rev. B* **39**, 11862.
- Ishimasa, T., H.-U. Nissen, and Y. Fukano, 1985, *Phys. Rev. Lett.* **55**, 511.
- Janner, A., and T. Janssen, 1977, *Phys. Rev. B* **33**, 2814.
- Kalugin, P. A., A. Y. Kitaev, and L. S. Levitov, 1985, *JETP Lett.* **21**, 145.
- Kelton, K. F., 1992, "Quasicrystals Structure and Stability," *Int. Mater. Rev.* (in press).
- Kelton, K. F., P. C. Gibbons, and P. N. Sabes, 1988, *Phys. Rev. B* **38**, 7810.
- Kelton, K. F., and J. C. Holzer, 1988, *Phys. Rev. B* **37**, 3940.
- Kimura, K., and S. Takeuchi, 1991, in *Quasicrystals: The State of the Art*, edited by D. P. DiVincenzo and P. J. Steinhardt (World Scientific, Singapore), p. 313.
- Klein, T., C. Berger, D. Mayou, and F. Cyrot-Lackmann, 1991, *Phys. Rev. Lett.* **66**, 2907.
- Koskenmaki, D. C., H. S. Chen, and K. V. Rao, 1986, *Phys. Rev. B* **33**, 5328.
- Kramer, P., and R. Neri, 1984, *Acta Crystallogr. A* **40**, 580.
- Kulkarni, U. D., 1989, *Phys. Rev. Lett.* **63**, 2484.
- Launois, P. M. Audier, F. Denoyer, C. Dong, J. M. Dubois, and M. Lambert, 1990, *Europhys. Lett.* **13**, 629.
- Levine, D., and P. J. Steinhardt, 1984, *Phys. Rev. Lett.* **53**, 2477.
- Levine, D., and P. J. Steinhardt, 1986, *Phys. Rev. B* **34**, 596.
- Levine, L. E., J. C. Holzer, P. C. Gibbons, and K. F. Kelton, 1992, *Philos. Mag.* **B 65**, 435.
- Libbert, J. L., K. F. Kelton, P. C. Gibbons, and A. I. Goldman, 1992, "Large Unit Cell Crystalline Approximant in Ti-Cr-Si," *J. Non-Cryst. Solids* (in press).
- Lubensky, T. C., 1988, in *Introduction to Quasicrystals*, edited by M. V. Jaric (Academic, Boston), p. 199.
- Lubensky, T. C., J. E. S. Socolar, P. J. Steinhardt, P. A. Bancel, and P. A. Heiney, 1986, *Phys. Rev. Lett.* **57**, 1440.
- Mackay, A. L., 1962, *Acta Crystallogr.* **15**, 916.
- Marcus, M. A., and V. Elser, 1986, *Philos. Mag.* **54**, L101.
- Mermin, N. D., 1992, *Rev. Mod. Phys.* **64**, 3; **64**, 635(E); **64**, 1163(E).
- Mizutani, U., Y. Sakabe, T. Shibuya, K. Kishi, K. Kimura, and S. Takeuchi, 1990, *J. Phys. Condens. Matter* **2**, 6169.
- Mott, N. F., 1987, in *Conduction in Non-Crystalline Materials* (Oxford University Press, New York).
- Mukhopadhyay, N. K., K. N. Ishihara, S. Ranganathan, and K. Chattopadhyay, 1991, *Acta Metall. Mater.* **39**, 1151.
- Mukhopadhyay, N. K., K. N. Ishihara, S. Ranganathan, and K. Chattopadhyay, 1985, *Scr. Metall.* **20**, 525.
- Mukhopadhyay, N. K., G. C. Weatherly, D. J. Lloyd, and J. D. Embury, 1992, "Synthesis and Characterization of Quasicrystals in a Rapidly Solidified Al-Fe-W Alloy," *J. Non-Cryst. Solids* (in press).
- Niizeki, K., and T. Akamatsu, 1990, *J. Phys. Condens. Matter* **2**, 2759.
- Pauling, L., 1985, *Nature* **317**, 512.
- Pearson, W. B., 1972, *The Crystal Chemistry and Physics of Metals and Alloys* (Wiley, New York).
- Poon, S. J., 1992, *Adv. Phys.* **41**, 303.
- Qiu, S. Y., and M. V. Jaric, 1990, in *Quasicrystals*, edited by M. V. Jaric and S. Lundqvist (World Scientific, Singapore), p. 19.
- Rabe, K. M., J. C. Phillips, P. Villars, and I. D. Brown, 1992, *Phys. Rev. B* **45**, 7650.
- Rabson, D. A., N. D. Mermin, D. S. Rokhsar, and D. C. Wright, 1991, *Rev. Mod. Phys.* **63**, 699.
- Ramachandrarao, P., and G. V. S. Sastry, 1985, *Pramana* **25**, L225.
- Robertson, L., and S. C. Moss, 1991, *Phys. Rev. Lett.* **66**, 353.
- Sainfort, P., B. Dubost, and A. Dubois, 1985, *C. R. Acad. Sci. Paris* **301**, 689.
- Shechtman, D., and I. Blech, 1985, *Metall. Trans. A* **16**, 1005.
- Shechtman, D., I. Blech, D. Gratias, and J. W. Cahn, 1984, *Phys. Rev. Lett.* **53**, 1951.
- Shield, J. E., C. Hoppe, R. W. McCallum, A. I. Goldman, K. F. Kelton, and P. C. Gibbons, 1992, *Phys. Rev. B* **45**, 2063.
- Socolar, J. E. S., and D. C. Wright, 1987, *Phys. Rev. Lett.* **59**, 221.
- Spaepen, F., L. C. Chen, S. Ebalard, and W. Ohashi, 1990, in *Quasicrystals*, edited by M. V. Jaric and S. Lundqvist (World Scientific, Singapore), p. 1.
- Stephens, P. W., and A. I. Goldman, 1986, *Phys. Rev. Lett.* **56**, 1168.
- Strandburg, K. J., L. Tang, and M. V. Jaric, 1989, *Phys. Rev. Lett.* **63**, 314.
- Torres, M., G. Pastor, J. Jimenez, and J. Fayos, 1989, *Philos. Mag. Lett.* **59**, 181.
- Tsai, A.-P., A. Inoue, and T. Masumoto, 1988, *Jpn. J. Appl. Phys.* **27**, L1587.
- Tsai, A. P., A. Inoue, Y. Yokoyama, and T. Masumoto, 1990, *Philos. Mag. Lett.* **62**, 95.
- Villars, P., J. C. Phillips, and H. S. Chen, 1986, *Phys. Rev. Lett.* **57**, 3085.
- Wang, N., H. Chen, and K. H. Kuo, 1987, *Phys. Rev. Lett.* **59**, 1010.
- Widom, M., D. P. Deng, and C. L. Henley, 1989, *Phys. Rev. Lett.* **63**, 310.
- Yang, Q. B., 1988, *Philos. Mag. Lett.* **57**, 171.
- Zhang, H., and K. H. Kuo, 1990, *Phys. Rev. B* **41**, 3482.
- Zhang, X., and K. F. Kelton, 1992, "High Order Crystalline Approximant Structures in Ti-Zr-Ni Alloys," *J. Non-Cryst. Solids* (in press).
- Zhang, Z., and K. F. Kelton, 1991, *Philos. Mag. Lett.* **63**, 39.

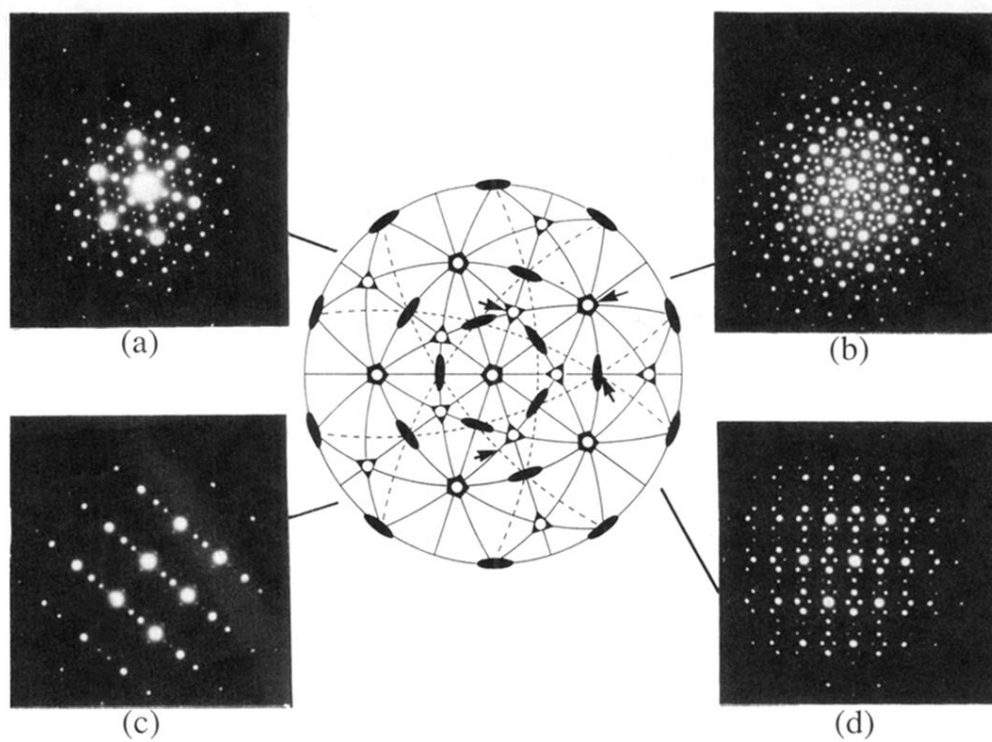


FIG. 1. Stereographic projection of the  $m\bar{3}5$  point group and accompanying TEM diffraction patterns from rapidly quenched Al-Mn taken perpendicular to a (a) a threefold axis, (b) a fivefold axis, (c) a pseudo-twofold axis, and (d) a twofold axis.

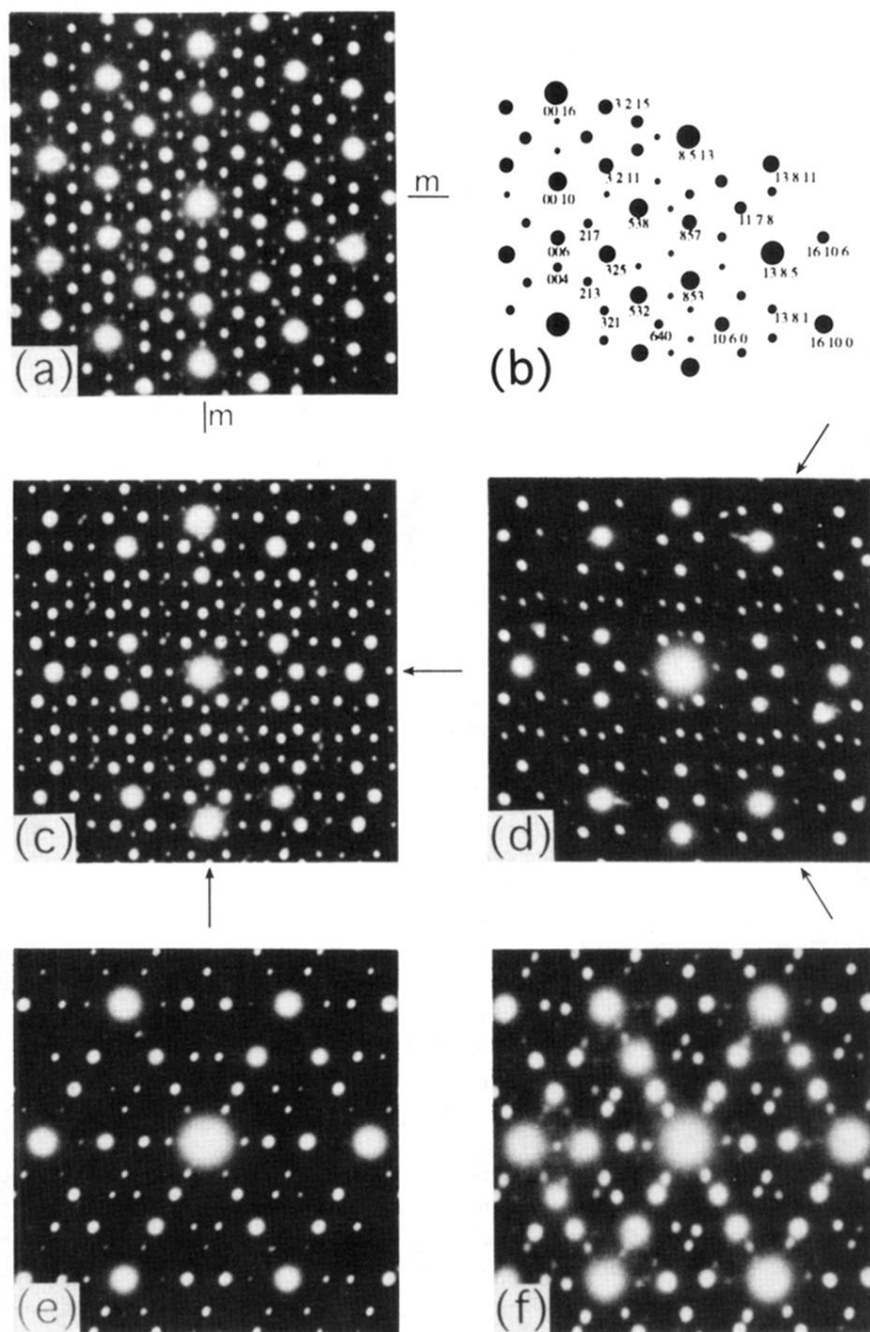


FIG. 10. Experimental selected area diffraction (SAD) patterns in  $\text{Ti}_{54}\text{Zr}_{26}\text{Ni}_{20}$ : (a) along the pseudo-fivefold axis; (b) an indexing of the pattern in (a) using cubic indices; (c) twofold axis along  $[100]$ ; (d) pseudo-twofold axes along other icosahedrally equivalent directions; (e) threefold axis along  $[111]$  of the cubic unit cell; (f) pseudo-threefold axis along other icosahedrally equivalent directions (from Zhang and Kelton, 1992).

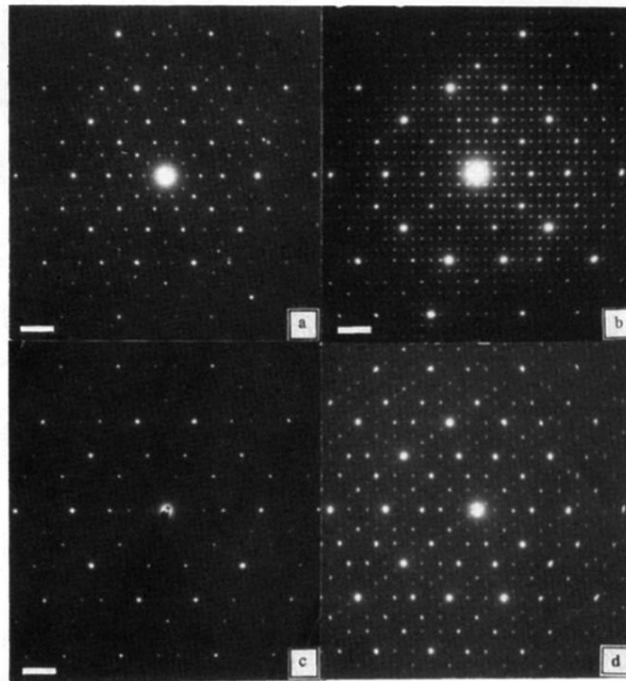


FIG. 11. Icosahedral fivefold and pseudo-fivefold diffraction patterns of the *i*-phase and three crystalline approximants in Ga-Mg-Zn: (a) *i*-phase; (b)  $3/2\text{-}2/1\text{-}2/1$  side-centered orthorhombic phase along the  $[110]$  zone axis; (c)  $2/1$  cubic phase along the  $[058]$  zone axis; (d)  $2/1$  rhombohedral phase along the  $[001]$  zone axis. The marker in the figure corresponds to  $1 \text{ \AA}^{-1}$  (from Spaepen *et al.*, 1990).

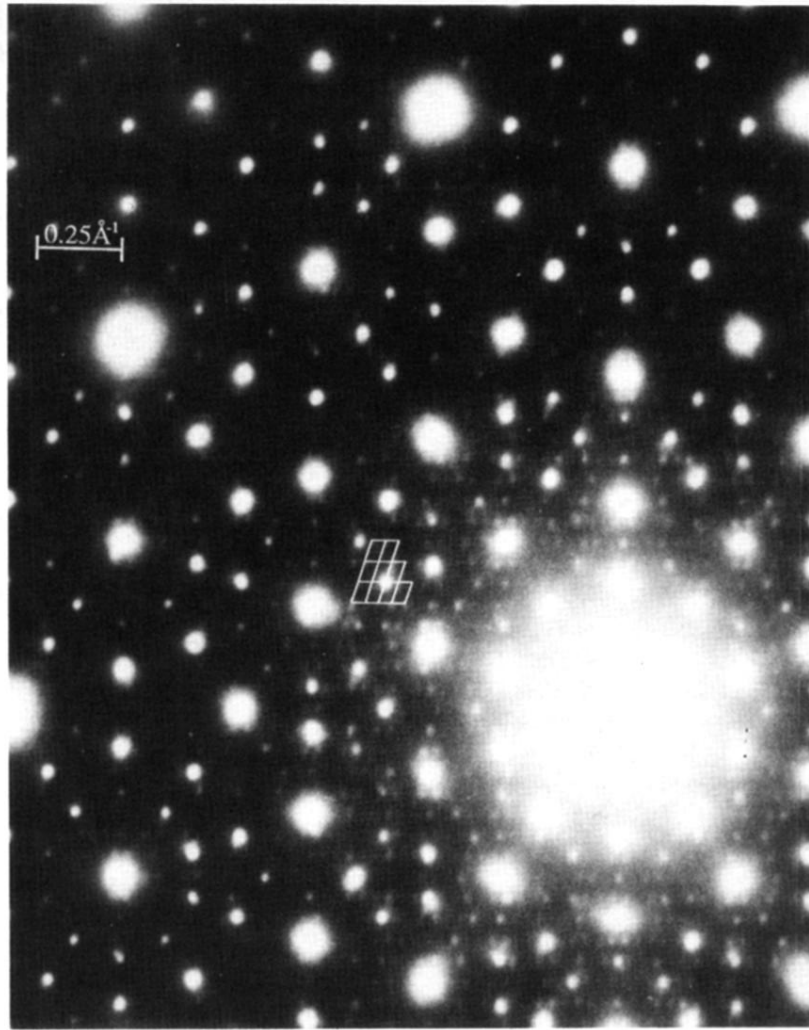


FIG. 12. Magnified region of a portion of the pseudo-tenfold selected area diffraction (SAD) pattern from decagonal  $\text{Al}_{64}\text{Co}_{22}\text{Cu}_{14}$  showing the periodic array of diffraction spots, corresponding to a repeat distance of about 100 Å (from Daulton and Kelton, 1992).

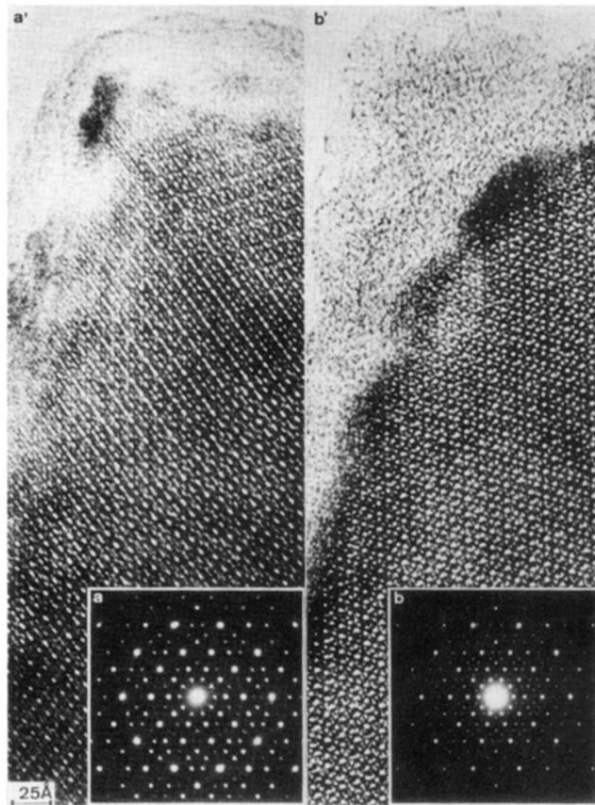


FIG. 13. Comparison of the electron diffraction patterns and high-resolution micrographs of the same area of an Al-Cu-Fe sample: (a) crystalline rhombohedral phase below 670 °C; (b) icosahedral quasicrystal above 670 °C (from Audier and Guyot, 1990).

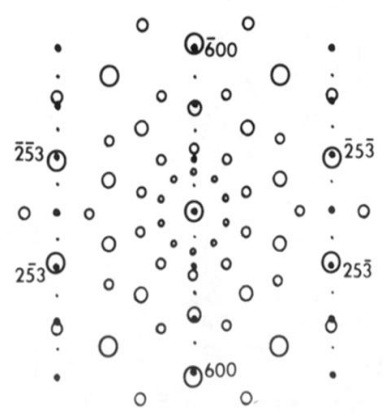
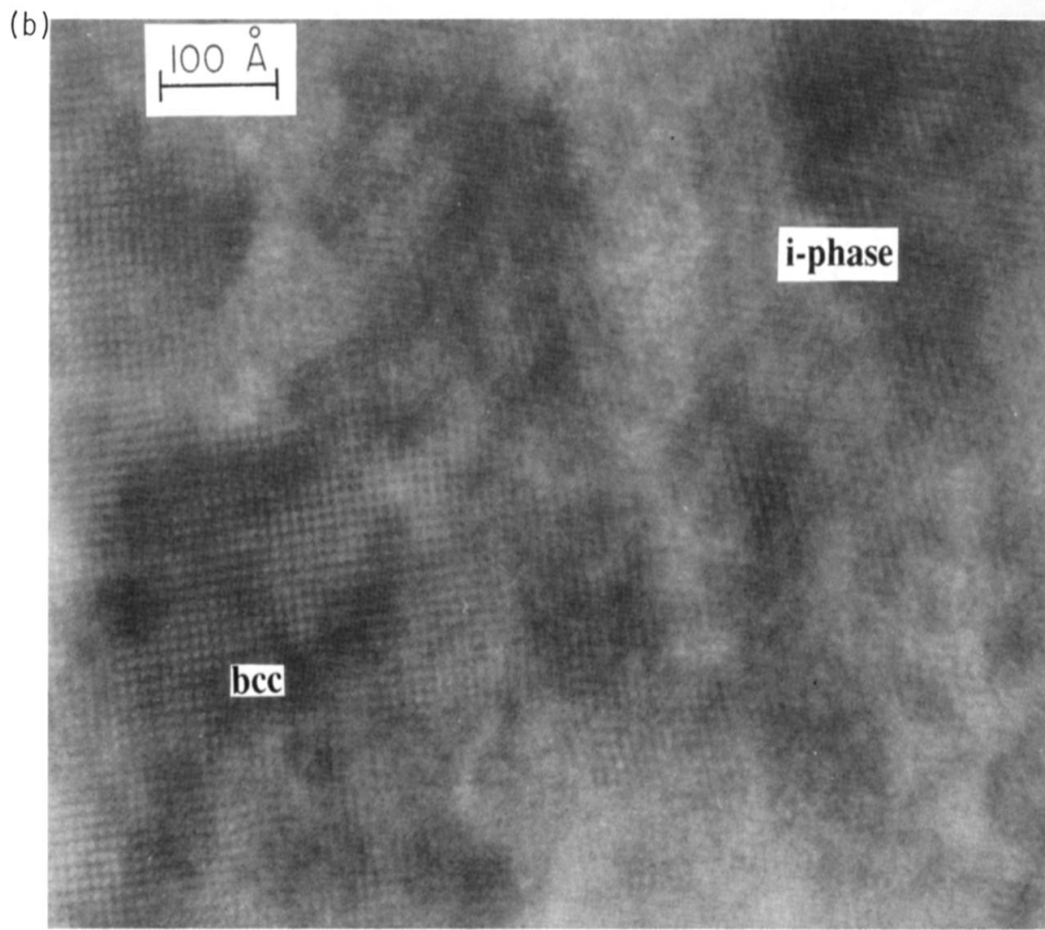
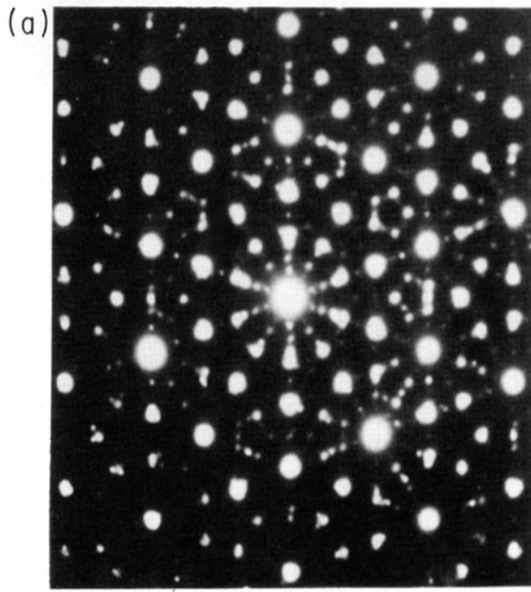


FIG. 4. Coherent orientational relationships between icosahedral phases and crystalline approximants. (a) Top: overlapping diffraction patterns of the fivefold zone of  $i(\text{AlMnSi})$  and the (530) zone of  $\alpha(\text{AlMnSi})$  (courtesy of H. S. Chen, taken from Koskenmaki *et al.*, 1986); bottom: schematic view of the top panel labeled with indices for the  $\alpha(\text{AlMnSi})$  diffraction spots. (b) High-resolution electron micrograph of coherent phase growth of the icosahedral and bcc phase of Ti-V-Si (from Zhang and Kelton, 1992).